NASA CONTRACTOR REPORT 177455

APPLICATION OF A COMPREHENSIVE ANALYTICAL MODEL OF ROTORCRAFT AERODYNAMICS AND DYNAMICS (CAMRAD) TO THE McDONNELL DOUGLAS AH-64A HELICOPTER

Cynthia B. Callahan
Duane E. Bassett

McDonnell Douglas Helicopter Company
Mesa, Arizona 85205

CONTRACTOR NO. A63622C

NOVEMBER 1988

National Aeronautics and
Space Administration

NASA CONTRACTOR REPORT 177455

APPLICATION OF A COMPREHANSIVE ANALYTICAL MODEL OF ROTORCRAFT AERODYNAMICS AND DYNAMICS (CAMRAD) TO THE McDONNELL DOUGLAS AH-64A HELICOPTER

Cynthia B. Callahan
D.E. Bassett

McDonnell Douglas Helicopter Company
Mesa, Arizona 85205

Prepared for
Ames Research Center
Under Contract No. A63622C
NOVEMBER 1988

National Aeronautics and
Space Administration

Ames Research Center
Moffett Field, California 94035

CONTENTS

LIST OF FIGURES

LIST OF FIGURES (Cont.)

LIST OF FIGURES (Cont.)

APPLICATION OF A COMPREHENSIVE ANALYTICAL MODEL OF ROTORCRAFT AERODYNAMICS AND DYNAMICS (CAMRAD) TO THE MCDONNELL DOUGLAS AH-64A HELICOPTER

By C.B. Callahan and D.E. Bassett
McDonnell Douglas Helicopter Company

SUMMARY

A model of the McDonnell Douglas Helicopter Company (MDHC) AH-64A helicopter was generated in a Comprehensive Analytical Model of Rotorcraft Aerodynamics and Dynamics (CAMRAD) in an effort to validate its analytical capabilities for modeling a current advanced Army helicopter. The initial phase of the effort involved the generation of the CAMRAD input files necessary for the complete aerodynamic, structural and dynamic definition of the production AH-64A helicopter. The input files were checked by making comparisons of CAMRAD full helicopter trim and main rotor blade natural frequency predictions with those of MDHC's full helicopter trim program, Blade Element Trim (BETRIM), and dynamic analysis code, Dynamic Analysis Research Tool (DART), respectively. The main thrust of the study concerned the application of the AH-64A CAMRAD model thus developed and verified for main rotor blade structural loads predictions and comparison with DART analytical results.

The study provided insight not only into the usefulness of CAMRAD for AH-64A performance and dynamics prediction, but also into the limitations of the program for modeling advanced rotor and fuselage systems. The general conclusion is that, despite the modeling limitations identified in the CAMRAD structural analyses, the structural loads predictions are as accurate as, and in some cases better than, analysis codes which provide more representative models of the complex geometries and structures of the AH-64A rotor system. However, it is apparent that the CAMRAD analysis in its current form cannot be considered fully reliable for dynamics predictions for more advanced rotor systems such as the bearingless rotor designs being proposed for LHX and future AH-64 configurations.

INTRODUCTION

Helicopter aeroelastic analysis is a complicated problem including complex rotor aerodynamics, rotor/fuselage interactional aerodynamics, rotor structural dynamics and rotor/fuselage coupled dynamics phenomena. An advanced and highly comprehensive analytical tool is necessary for effectively representing these phenomena to provide accurate predictions of the aerodynamics and dynamics properties of rotorcraft systems. Two additional goals in the development of any analytical tool are that it be computationally

efficient and sufficiently general so that it can be applied to a variety of rotorcraft configurations with little or no modification necessary to the basic model.

CAMRAD (references 1, 2, and 3) provides the kind of comprehensive, efficient and general analytical rotorcraft model necessary to effectively perform the complex task of helicopter rotor aerodynamics and structural dynamics prediction. The program, developed by Wayne Johnson at the National Aeronautics and Space Administration (NASA) Ames Research Center, comprises structural, inertial, and aerodynamic models that extensively define the helicopter for determination of rotor performance, loads, and noise, and helicopter vibration, flight dynamics and aeroelastic stability. It is applicable to a wide variety of rotorcraft configurations and a broad class of problems.

Presented herein are the results of comparisons of CAMRAD trimmed level flight performance, main rotor blade natural frequency, and main rotor blade structural loads predictions for the AH-64A helicopter with the predictions of MDHC analytical tools and flight test data. Conclusions are drawn about the general applicability of CAMRAD for AH-64A performance and structural dynamics predictions. In addition, the characteristics of the AH-64A helicopter pertinent to the accurate modeling of the aircraft are also described and the dynamics and performance analysis programs used for comparison are discussed.

THE MDHC AH-64A HELICOPTER

A three view schematic of the MDHC AH-64A helicopter is shown in figure 1. The main rotor of the AH-64A is a four-bladed, fully articulated system with a tip radius of 288 inches and an operational rotor speed of 289 revolutions per minute. The blade attachment point is 39 inches from the center of rotation. The blade planform is rectangular between radial station 81 inches and 268 inches with a chord of 21 inches. From radial station 268 inches, the trailing edge is swept linearly aft 20 degrees to the tip. The chord of the swept tip is 21 inches as measured perpendicular to the leading edge. The main rotor blade section is an HH-02 airfoil with a thickness ratio of 9.5 percent which extends from blade station 82 inches to 268 inches. The airfoil incorporates a 10 percent trailing edge tab which is deflected trailing edge upward by 5 degrees. The section transitions to a NACA 64A006 airfoil at the tip. The rotor blade has a built-in linear twist of -9 degrees. A schematic of the blade planform is shown in figure 2.

The main rotor hub, shown schematically in figure 3, is a complex configuration utilizing retention straps composed of thin steel laminates to provide a structural tie between the blade and the hub. The basic function of the retention straps is to carry the blade centrifugal force and at the same time permit flapping and feathering motions without the need for heavily loaded bearings. The straps are encased by a pitch housing which is attached to the hub via a flap/feather bearing located at 11.0 inches from the center of rotation. The pitch case and straps are attached to the blade at the lead-lag link located 34.5 inches from the center of rotation. The pitch case and strap system forms a structural redundancy for carrying blade loads into the hub. Elastomeric lead-lag dampers, located

along either side of the pitch housing, provide damping restraint of lead-lag motions, thus eliminating aeromechanical instability and coupled pitch-flap-lag instability.

The teetering tail rotor is four-bladed with a radius of 4.58 feet. The configuration is that of two two-bladed teetering rotors stacked one on the other such that one blade pair is at an angle of 60 degrees to the other. The tail rotor airfoil is a modified NACA 63A410.

The AH-64A fuselage incorporates a stub wing with a semispan of 98 inches and a fixed incidence angle of 6 degrees with respect to the fuselage waterline. The wing supports a variety of weapons stores in addition to external fuel tanks for long range missions. The horizontal stabilator has a semispan of 66.9 inches. Stabilator incidence varies as a function of airspeed and collective stick input from 25 degrees nose up in hover to -5 degrees in forward flight.

The AH-64A helicopter has an operating gross weight range of 11,600 to 21,000 pounds and a center of gravity range from fuselage station 200 to 207 inches.

MDHC ANALYSIS PROGRAMS

MDHC's primary performance analysis program, Blade Element Trim (BETRIM), provided the baseline for the aircraft performance comparisons. Lifting Surface Axial Flow (LSAF) was also used to provide additional comparison for hover performance. Dynamic Analysis Research Tool (DART) served as the baseline for the main rotor blade natural frequency and structural loads comparisons. These programs have been used extensively for AH-64A performance and dynamics analyses at MDHC and are discussed below.

Blade Element Trim - BETRIM

BETRIM (reference 4) is an analytical computer program developed at MDHC which calculates performance characteristics for a conventional single main rotor helicopter in trimmed level flight and in quasi-steady maneuvers. It trims the full helicopter in 6 degrees of freedom using main rotor collective, longitudinal cyclic and lateral cyclic pitch; fuselage pitch, yaw or roll attitudes; and tail rotor collective pitch.

The main rotor rigid blade model uses lifting line blade element theory in conjunction with a table lookup scheme for airfoil lift, drag and pitching moment characteristics. The program linearly interpolates airfoil coefficients over specified airfoil transition regions such as that of the AH-64A swept tip. Lifting line theory is enhanced by the use of a tip loss correction which parabolically reduces the blade section lift to zero at the tip from its uncorrected value at a station calculated as a function of blade aspect ratio. Mach number is corrected for compressibility effects at the tip by applying a reduction factor which is a function of chord and radial station. Effective blade section angle of attack is corrected for unsteady aerodynamic effects by modification as a function of pitch rate and local velocity. Dynamic stall effects are simulated by the use of extended lift coefficient data. The section aerodynamics calculations include the effects of radial drag and yawed flow.

BETRIM utilizes a simple nonuniform first harmonic inflow model based on momentum theory. Empirical corrections may be applied to simulate the effects of nonuniform inflow, tip losses, etc. The program can also incorporate a rigid or free wake inflow model based on that developed by G. Hartwick and S. Sadler at Rochester Applied Science Associates, Inc. (reference 5).

Tail rotor aerodynamic characteristics are provided by a table lookup scheme for determination of the tail rotor collective pitch required to produce the desired anti-torque thrust. Fuselage aerodynamic data is provided in table form for the fuselage, wing and horizontal and vertical stabilizers individually. Additional flat plate drag area may be input in order to account for drag due to other fuselage appendages, such as different wing store configurations and instrumentation required for test measurements. BETRIM also incorporates the capability for calculating the horizontal stabilator schedule as a function of collective pitch and airspeed.

Lifting Surface Axial Flow - LSAF

LSAF is a state-of-the-art hover/axial flight performance prediction code developed by J. D. Kocurek (reference 6). The analysis is based on lifting surface theory and uses a circulation-coupled prescribed wake model for calculation of induced velocity distributions. The code offers a refined 3-D compressibility model, airframe download model, and off-disk velocity field capability. It has been successfully correlated with a wide variety of rotor planforms, tip shapes, and twist distributions. MDHC has correlated LSAF hover performance results with AH-64A hover test data with good results.

Dynamic Analysis Research Tool - DART

DART (reference 7) is a general finite element structural dynamics program developed by the MacNeal-Schwendler Corporation. It has been updated and maintained by MDHC since 1965 and has proved to be effective in application. The program is used for vibration, loads, aeroelasticity and mechanical stability investigations of rotor systems.

DART performs four basic types of analyses on systems having up to 110 degrees of freedom: 1) real eigenvalue analysis, 2) complex eigenvalue analysis of fully coupled linear equations of motion, 3) frequency response analysis, and 4) transient response analysis to time-varying forced excitations including nonlinear effects. The program generates and solves the set of equations that describes a finite element model of a structure. The model may consist of four basic types of elements: mass, damper, stiffness and constraint elements. A flow chart of the DART program is shown in figure 4.

Some special features of the DART rotor analysis include:

a. Structural Preprocessors. The DART program incorporates structural preprocessors which convert blade structural data into finite elemental properties. The preprocessors calculate finite element values which represent all significant dynamic coupling effects between flapwise bending, chordwise bending and twist. The couplings modeled are

those due to center of gravity offset, shear center offset, steady blade pitch and twist, and steady blade vertical and inplane bending.

b. Retention System Modeling Flexibility. DART has the ability to add conventional structural elements, which represent the properties of the retention system and of other components such as tuned absorbers, to the elements calculated by the blade structural preprocessors.

c. Bearingless Rotor Modeling. The DART analysis is well suited for hingeless and bearingless rotor dynamics modeling. This is because of the inherent flexibility in DART to accurately model the structural characteristics of the flexible strap, the redundant load path in the torque tube, and the flap-lag, pitch-lag and flap-pitch kinematic couplings through constraint relationships.

d. Structural Coupling. Structural coupling effects are linearized in the eigenvalue analysis as follows: flap-lag coupling due to geometric pitch is based on built-in twist plus steady collective pitch, neglecting cyclic pitch and structural twist due to applied loads. Pitch-flap-lag coupling due to flapwise bending is based on the mean deflected shape corresponding to the given steady thrust, collective pitch, and inflow condition, neglecting oscillatory deflections due to unsteady airloads. These nonlinear effects are included in the transient analysis.

e. Nonlinear Aerodynamics. The DART transient analysis permits use of a nonlinear formulation of the aerodynamic coefficients (nonlinear lift, drag and moment coefficients as arbitrary functions of angle of attack, Mach number, and spanwise station); it also accounts for dynamic stall and sweep effects, including lift and moment hysteresis on the aerodynamic forces. In addition, the nonlinear coupling effects mentioned in the preceding paragraph are included. The program utilizes either constant inflow or time- and radially-varying inflow as prescribed by the user.

f. Rotor Trim. DART incorporates a routine that simulates an autopilot in order to produce a desired steady-state trim condition with prescribed flapping, thrust, and/or shaft torque. This is accomplished by supplying cyclic or collective pitch inputs and/or inflow. DART trims the rotor for steady forward flight by numerically integrating the nonlinear equations of motion for a sufficiently long time for initial transients to die out and for the autopilot to achieve the desired trim condition.

APPROACH

The basic approach taken, from initial development of the CAMRAD AH-64A model to the generation of the results presented here, is discussed below. The evolution of the physical model definition in CAMRAD is described. The basic analytical models used in the analysis programs applied for each particular study are also discussed. Finally, a description of the flight test data used in the comparisons is provided.

Model Development

The generation of the numerous CAMRAD inputs necessary for the complete physical definition of the AH-64A helicopter required a considerable effort. Much care was taken to ensure that the physical model data were accurate and consistent with those of the MDHC analysis programs used for comparison. Particular emphasis was placed on the accurate definition of the AH-64A main rotor system in CAMRAD. During the model generation process, however, several limitations inherent in the CAMRAD rotor structural analysis were found to be somewhat restrictive for the AH-64A. These restrictions resulted in a rotor structural model in CAMRAD which was not entirely consistent with that of DART or the actual rotor configuration. The specific limitations encountered in the CAMRAD blade structural analysis are as follows.

1. In the absence of blade droop or sweep at the location of the pitch bearing, the undeformed elastic axis is a straight line and is necessarily coincident with the feathering axis.
2. For analysis of inplane degrees of freedom, the structural analysis assumes the blade to be cantilevered at the lead-lag hinge.
3. There is no provision for modeling structural redundancies.

As shown in figure 2, the elastic axis of the AH-64A main rotor blade is not only swept at the tip but is coincident with the feathering axis only over a very small section at the root end of the blade. Over the constant portion of the blade from radial station 82 to 268 inches, the elastic axis is forward of the feathering axis by approximately 1.5 inches. It is therefore not possible to correctly represent both the elastic and feathering axes in CAMRAD. It was demonstrated using DART that the accuracy of the elastic axis location is less important than that of the feathering axis. Therefore, the feathering axis and all cross-section offsets other than the shear centers were correctly represented in the CAMRAD model. The elastic axis was consequently modeled as coincident with the true feathering axis. The impact of this inconsistency was investigated and is discussed in a later section.

The assumption of rigidity inboard of the lag hinge is also not entirely valid for the AH-64A. Inplane rotation is permitted at the spherical flap/feather bearing because the strap pack, even under centrifugal stiffening, is not rigid in the lead-lag direction. This problem revealed itself in the CAMRAD prediction of a first elastic inplane mode which was approximately 0.4 per revolution higher than the DART prediction at 100 percent rotor speed. To demonstrate the source of this discrepancy, the effect of strap pack inplane flexibility inboard of the lag hinge was removed from the DART model. The inplane mode prediction using this modified model was comparable to that of CAMRAD. To improve the inplane mode correlation, an attempt was made to simulate the strap inplane flexibility in CAMRAD by moving the lead-lag hinge point inboard until the first elastic chordwise bending mode showed agreement with the DART prediction. This required a hinge offset of 9.15 percent as opposed to the physical hinge offset of 11.98 percent. It was necessary

to readjust the lead-lag hinge spring stiffness in order to bring the rigid lag mode back to the correct value. The modified hinge parameters were used in the baseline CAMRAD AH-64A model and are thus represented in the results shown in following sections.

The inability of CAMRAD to model structural redundancies is not considered to be as significant a problem for AH-64A structural blade loads prediction. However, it should prove to be more limiting for fuselage vibration prediction.

In addition to defining the basic AH-64A physical model, it was necessary to determine the types of analyses to be run and to select the various options available in each analysis program. Studies were performed to investigate the usefulness of several of the CAMRAD analytical options. The general approach, however, was to make the CAMRAD analyses basically consistent with those of the MDHC analysis programs in order to get a more direct comparison of the basic mathematical models used in each code.

The physical and analytical modeling configurations which were determined to provide the best representation of the AH-64A for the analyses performed in the present study are described below.

Full Helicopter Trim Prediction

CAMRAD provides several user options for the analysis of rotor aerodynamics. CAMRAD's first harmonic momentum-based inflow model was used as was a similar model in BETRIM. Radial drag effects were included but yawed flow corrections were not used. The McCroskey dynamic stall model without vortex loading effects (reference 1) was employed and unsteady lift and moment contributions were also included. Tip loss based on the Prandtl function (reference 1) was used but tip relief factors were not applied. CAMRAD does not provide a model for a four-bladed teetering tail rotor. For these studies, the articulated rotor model was used and hinge offsets were placed at the hub centerline.

Main Rotor Natural Frequency Prediction

Prior to generation of the structural loads results, the basic rotor structural model in CAMRAD was checked by making comparisons of rotating blade natural frequencies with those of DART. CAMRAD's flutter analysis was used to predict the rotating blade natural frequencies *in vacuo*. The analysis predicts up to 10 fully coupled flap and lead-lag bending modes and 5 fully coupled torsion modes for a single blade using an isolated blade analysis. The blade and hub structural properties used in the AH-64A CAMRAD model were made consistent with those used in the DART model with those exceptions noted above.

Main Rotor Blade Structural Loads Prediction

Elastic blade analysis was used in CAMRAD for the loads predictions. Six bending modes (two edgewise and four flapwise) and two torsion modes (rigid and first elastic) were

used, thus including main rotor blade resonances up to 10 per revolution. Ten harmonics of rotor motion were retained in the analysis. Due to the importance of wake effects on blade loading, CAMRAD's prescribed wake analysis was employed for the comparisons. CAMRAD's dynamic stall options were implemented in the initial studies but circulation convergence problems precluded their continued use. Therefore, static stall was used exclusively for the loads predictions. Simple tip loss was also employed in place of the Prandtl function tip loss that was used for the trim comparisons.

In order to eliminate possible inconsistencies due to fuselage aerodynamics, CAMRAD loads were generated using the isolated rotor model. The longitudinal shaft tilt was set equal to the total shaft tilt exhibited in flight test. The rotor was trimmed to propulsive force and thrust using collective and longitudinal cyclic pitch. Lateral cyclic pitch was held fixed at the flight test value.

Loads predictions were made for the same flight conditions using the DART analysis for comparison. DART requires the trimmed cyclic flapping angles, thrust and inflow as input. It trims the rotor to the input thrust and first harmonic flapping by adjusting collective and cyclic pitch. To provide maximum comparability between the DART and CAMRAD results, the CAMRAD first harmonic flapping, thrust and induced velocities in the plane of the disk were input to DART. The intent was to eliminate some of the aerodynamics variables from the predictions to provide a more direct comparison of the structural analyses.

Flight Test Data

The test data used in the study were obtained from flight tests of Production Vehicle - 01 conducted between 1984 and 1986. The measured performance data used for the comparisons include shaft torque, control actuator positions, main rotor shaft attitude and flapping and lead-lag angle measurements. Main rotor shaft torque and attitude measurements were found to be generally consistent between similar tests. Control actuator position was determined to give the most accurate indication of pilot control input. The flap and lag angular measurements were suspect and thus were used only to provide a qualitative feel for general trends in trim state with flight speed.

Rotor blade structural load instrumentation included six flap bending gages at 46, 103, 174, 222, 246 and 260 inches; three chordwise bending gages at 103, 174 and 260 inches; and two torsion gages at 104.5 and 260.5 inches from hub centerline. Moment data were selectively chosen by examining trends with level flight and radial station and discarding data from tests which did not follow trends defined by the majority of the data. Accepting some scatter due to the ranges of gross weight, fuselage configuration and air density, the trends in blade structural loads are, in general, well defined and provide a good level of confidence in the test data.

RESULTS AND DISCUSSION

Basically independent sets of results were generated using three CAMRAD analyses: full helicopter trim, flutter and isolated rotor trim. The CAMRAD analytical predictions were compared to those of other analysis programs and to flight test data. The results of each of these studies are described below.

Full Helicopter Trim Predictions

CAMRAD trim predictions were made for the AH-64A in hover and in level flight at 60, 100, 140 and 154 knots true airspeed at a pressure altitude of 4000 feet and a temperature of 95 degrees Fahrenheit. The results of the level flight trim comparisons are shown in figures 5 through 15 as main rotor shaft horsepower required, fuselage pitch and roll attitudes, and main rotor steady and cyclic feathering, flapping and lead-lag angles, respectively. Flight test data are included, where available, for additional comparison. It is of note that for the 154-knot trim analysis, full helicopter trim was not achieved in CAMRAD with the application of the dynamic stall model. The reasons for this problem are as yet unresolved. As a result, static stall was used for this case.

In general, the BETRIM and CAMRAD results show good agreement. Overall discrepancies can be traced to differences in the rotor advanced aerodynamic modeling capabilities available in the two models such as unsteady aerodynamics and dynamic stall. Further differences arise due to the fact that CAMRAD does not interpolate airfoil data as does the BETRIM program. It is, of course, possible to create additional airfoil tables for the transitioning airfoils for use in CAMRAD by externally interpolating the data. Another probable cause for differences may be the spanwise airload integration methods used by the two programs. BETRIM uses a Simpson's rule integration scheme whereas CAMRAD uses step integration.

Figure 5 shows main rotor shaft torque predictions versus flight speed for CAMRAD and BETRIM in comparison with test measured values. The analytical predictions are comparable but both are considerably higher than the measured values, particularly for flight speeds in the middle of the speed range, with correlation improving at the higher speeds. Analytical predictions of fuselage pitch attitude (figure 6a) are comparable at the lower speeds but begin to diverge slightly at 100 knots. It is thought that differences in the CAMRAD and BETRIM aerodynamic interference calculations resulted in discrepancies in the calculated effective angle of attack of the horizontal tail thus resulting in differences in calculated stabilator lift and consequently in fuselage pitch attitude. The agreement of both analyses with test data is fair. Predicted fuselage roll attitude, shown in figure 6b, is comparable between the two programs.

Main rotor collective pitch (figure 7) is fairly well predicted by both analyses, with correlation with test decreasing at the higher speeds. Longitudinal and lateral cyclic pitch (figures 8 and 9) are not well predicted by either analysis. Correlation of CAMRAD longitudinal cyclic pitch predictions improves at the higher speeds.

The coning predictions, shown in figure 10, are comparable between CAMRAD and BETRIM. Perhaps the most significant difference in the trim states is in longitudinal flapping (figure 11). This is reflected in the differences in fuselage pitch attitude and longitudinal cyclic pitch predictions between CAMRAD and BETRIM. Lateral flapping predictions (figure 12) are comparable. The lag response of the AH-64A rotor is very low and BETRIM and CAMRAD predictions are similar (figures 13,14 and 15).

Hover performance predictions generated by CAMRAD were also compared to LSAF predictions in the form of C_Q versus C_T. LSAF provides a more accurate model for hover performance analysis than does BETRIM, primarily due to the hover prescribed wake model available in LSAF. Results are shown in figure 16. Test data are also provided for comparison. As seen in figure 16, CAMRAD hover performance predictions agree very well with the LSAF results. It is thought that the empirical corrections made to the simple nonuniform inflow model used in CAMRAD provided the extra degree of correlation.

Main Rotor Natural Frequency Predictions

The resonance diagram comparing the CAMRAD and DART predictions based on the CAMRAD input modifications discussed in a previous section is shown in figure 17. CAMRAD predictions show good agreement with the DART results up to frequencies of eight per revolution. The discrepancy in the third elastic flapwise bending mode at the higher rotor speeds and the significant difference in the second elastic torsion natural frequency over the entire rotor speed sweep have yet to be resolved.

Main Rotor Blade Structural Loads Predictions

AH-64A main rotor blade structural loads were predicted using CAMRAD for hover out of ground effect and 80, 100, 140 and 154 knots true airspeed in level flight. The results of comparison of these predictions with DART and test measured data are discussed below for trim as well as blade structural loads.

Isolated Rotor Trim Comparisons

Figures 18 through 20 show main rotor shaft torque, collective pitch, and longitudinal cyclic feathering, respectively, versus forward speed for DART, CAMRAD and flight test data. As seen in figure 18, the CAMRAD main rotor shaft torque prediction is consistently higher than the measured values over the range of airspeeds studied. Correlation improves to some extent at the higher speeds. The same trend was visible in the full helicopter trim predictions using uniform inflow and rigid blade analyses (figure 5). A potential source of the discrepancy is the two-dimensional airfoil data. However, the DART shaft torque predictions, which utilized the same basic airfoil data, agree much better with the test measured values over the lower end of the speed range (figure 18).

As seen in figure 19, the CAMRAD collective pitch predictions are also on the high side of the test data scatter. Examination of the steady torsional moment predictions in

comparison with test (figure 27a) indicate more nose-down torsional bending predicted by CAMRAD as compared to test at the lower speeds with correlation improving at 140 knots. The excessively nose-down deformation is thought to be due at least in part to the more aft than actual chordwise offset of the aerodynamic center from the elastic axis over the entire blade and in particular at the blade tip resulting from the modeling limitation in the CAMRAD blade structural analysis discussed previously. DART also slightly over-predicts collective pitch at the lower speeds, but to a lesser extent than CAMRAD. DART underpredicts the collective requirement at the higher end of the speed range. However, DART consistently shows a more nose-down steady torsional moment than CAMRAD over the entire speed range examined.

As shown in figure 20, longitudinal cyclic feathering is well predicted by both DART and CAMRAD as compared to the test measurements over the entire speed range studied. This is a good indication that the shaft attitude input into the two isolated rotor programs is consistent with that actually exhibited in test.

Structural Loads Results

The results of the structural loads comparisons are shown in figures 21 through 29 for level flight at 100 knots true airspeed. These plots are in the forms of distributions of steady and cyclic flapwise, chordwise and torsional bending loads along the radius and time histories of vibratory loading in the three directions at 36 percent radius. For the time history comparisons, the steady components were removed to provide more visibility to the vibratory results. A similar set of figures is provided in Appendix A for the hover and 80, 140 and 154 knots flight conditions. Also shown below are variations in steady and cyclic load at 36 percent radius with airspeed.

Flap bending.

In general, steady flap bending moments, shown in figure 21a, are very well predicted by both DART and CAMRAD at 100 knots over the majority of the radius. There are more significant discrepancies at the blade root between the two analyses and the test measurements with CAMRAD showing a much sharper increase in bending at the root than predicted by DART. In this region of the blade at the lead-lag hinge (0.12R), the flapwise stiffness increases very rapidly. The method employed in CAMRAD for calculation of structural loads from curvature and stiffness is not expected to be reliable in regions such as this where large changes in stiffness occur. The cyclic flap predictions (figure 21b) are also in good agreement for the two analyses and correlate fairly well with test data over the midspan with correlation worsening at the outboard regions and at the root.

The time history of vibratory flap bending at 36 percent radius (figure 22) shows very good agreement in the DART and CAMRAD predictions and fair correlation with the test measured loading. Aerodynamic loading dominates the out-of-plane vibratory response and thus the more general differences in the structural loads predictions are thought to arise from inaccuracies in the aerodynamics predictions, particularly in the higher harmonics. Correlation between the CAMRAD time history results and test data is comparable at 60 percent radius.

The trend of steady flap at 36 percent radius with flight speed shown in figure 23a shows poor correlation with test data for both codes over the entire speed range. Cyclic flap moment trends with airspeed (figure 23b) are much better predicted by both programs.

Chord bending.

Steady chordwise bending moment for the 100 knots flight condition is shown in figure 24a as a function of radial station. The CAMRAD prediction shows fair agreement with the limited number of test data points available. The gross underprediction of steady chordwise bending by DART has not been explained. The CAMRAD cyclic chord bending radial trend (figure 24b) is somewhat unusual but provides a moderate level of correlation with the measurements at the two radial stations at which data was available. Again, the DART prediction is considerably lower than CAMRAD or test.

As shown in figure 25, the chordwise bending time history predictions of both analyses correlate poorly with the test measured data. As is apparent from the figure, the AH-64A cyclic chordwise loads are predominated by the fourth harmonic resulting from drive train dynamics. Neither analysis utilized for this study included a drive train model. An attempt was made to include drive train dynamics in CAMRAD, but little significant effect was seen in any of the loads results. The level of correlation does not improve significantly at 60 percent radius.

The trends of chord bending with forward speed are shown in figures 26a and b. The trend in steady chord moment exhibited by the test data shows a steady decrease in load with speed from about 100 knots. The CAMRAD prediction, however, shows increasing moment with speed out to 140 knots with some decrease between 140 and 154 knots. The CAMRAD cyclic chord bending prediction (figure 26b) agrees much better with the test measurements. The DART predictions are considerably below the test-measured levels for both steady and cyclic loading.

Torsion.

Figure 27a shows steady torsional moment versus radius for the 100 knots flight condition. Both the CAMRAD and DART predictions are excessively nose-down in comparison with test data. The erroneous shear center offsets relative to the centers of gravity and the aerodynamic centers as modeled in CAMRAD are expected to effect the torsional moment predictions to some extent. In particular, the greater than actual offsets of the aerodynamic centers with respect to the shear centers in the swept tip region of the blade result in a larger nose-down aerodynamic moment prediction in the tip region. CAMRAD does, however, predict the nose-up moment displayed by the test data at the tip. Cyclic torsional moment predictions (figure 27b) are comparable between both programs but are consistently less in magnitude than test data over the blade span.

As seen in the vibratory time history comparison in figure 28, the predictions of both codes are quite different and neither agrees well with test data. The degree of correlation is worse at 60 percent radius.

Figure 29a provides a comparison of the analytical predictions and test data trends of steady torsion at 36 percent radius with forward speed. There is a fairly constant

delta between the DART and CAMRAD predictions between 80 and 100 knots and both predictions are more nose-down than exhibited by test. Moreover, the test measured data shows a greater rate of increase with speed than the analytical predictions. The trend in cyclic torsion with flight speed is shown in figure 29b. The DART and CAMRAD predictions are in good agreement between 80 and 140 knots but neither analysis predicts the magnitudes or the steeper trend shown in the test data.

Investigation of the Effects of Structural Offsets

As described in a previous section, the CAMRAD structural analysis exhibits several particular modeling limitations when applied to the AH-64A rotor system. Perhaps the most uncertainty in the CAMRAD structural loads predictions for the AH-64A rotor blade arise as a result of the restrictions on elastic axis modeling inherent in the CAMRAD blade structural model. Because it is not possible to correctly represent all blade structural offsets in CAMRAD, it was necessary to determine the most representative blade model in terms of offsets defined within the analytical modeling constraints.

The offsets of the centers of gravity with respect to the aerodynamic centers have a significant effect on torsional loads. Similarly, the offsets between the tension centers and centers of gravity must be correct for accurate chordwise loads prediction. In addition, it is necessary for the center of gravity offsets from the center of rotation to be correct for accurate representation of the line of action of the centrifugal force which predominates the steady chordwise loads. Thus, these three offsets must maintain their actual physical locations on the blade in order to provide the most accurate loads predictions.

Torsional loads also depend to a large extent on the offsets from the shear centers to the centers of gravity and aerodynamic centers. However, when maintaining the correct relative distance between the aerodynamic centers and centers of gravity, the incorrect offset between these points and the shear centers is thought to be somewhat corrected by the canceling effects of the changes in the aerodynamic and inertial moments about the shear center.

In order to determine the importance of an accurate representation of the elastic axis, DART was employed to run a model of the AH-64A blade in which the elastic axis was represented as in the CAMRAD model, as a straight line coincident with the feathering axis. Although it is recognized that the effect demonstrated by the modified DART model is somewhat dependent on the particular theory and mathematical model employed in the code, the fairly significant differences in the loads predictions between the two models does cast some doubt on the complete effectiveness of CAMRAD in its present form for AH-64A blade loads prediction.

Inclusion of Additional Degrees of Freedom

The baseline CAMRAD model utilized in the studies discussed above included 6 bending and two torsion modes in the blade structural analysis. Studies were performed to show the effect of the inclusion of additional bending and torsion degrees of freedom on blade structural loads prediction. To demonstrate the effects of the higher torsion modes, loads

were predicted using CAMRAD with 6 bending and 3 and 5 torsion modes, respectively. Neither increase effected the loads predictions significantly. To show the effects of the higher frequency bending modes, predictions were made using 8 bending and the baseline 2 torsion modes. The most apparent differences produced were in the cyclic flap and chord loads, but these were minor and did not effect the overall level of correlation with test data. Finally, predictions were made using the maximum number of modes: 10 bending and 5 torsion. Torsion was essentially uneffected. Steady and cyclic flap and cyclic chord showed only minor differences. The most dramatic changes were seen in the steady chord radial distribution. However, with the limited number of test data points available, it was difficult to determine if the level of correlation was altered. The solutions did not appear to be converging with increasing number of modes. The performance and trim predictions were entirely uneffected by any combination of the degrees of freedom. It is of note that the eighth bending and third torsion modes are both above 15 per revolution and although these higher modes do effect the solution, their accuracy has not been verified.

CONCLUSIONS

Correlation studies are necessary before any analytical tool can be used with confidence for prediction of the behavior of a physical system. Successful correlation with a variety of configurations can provide confidence in the analytical predictions for similar systems in the design phases of development. Much was learned during the investigations presented here about CAMRAD's capabilities and limitations for modeling the AH-64A helicopter. This information can be extrapolated to determine CAMRAD's applicability for modeling similar rotor and fuselage systems.

The following general comments are made regarding these investigations of CAMRAD for AH-64A analysis.

Full Helicopter Trim Comparisons

In general, CAMRAD offers an advanced and considerably versatile performance analysis, particularly in the analysis of rotor aerodynamics. The scope of the present effort did not allow for the full exploration of all the CAMRAD modeling options available. It is thought that a more comprehensive study of full helicopter trim analysis using CAMRAD with more extensive correlation with test data would result in much more acceptable correlation.

There are several relatively minor limitations in the CAMRAD aerodynamics models, the most general of which is that CAMRAD does not provide the capability for spanwise interpolation of airfoil characteristics within the program computational sequence. It is possible, however, to interpolate the tables externally and use the additional tables in CAMRAD for the transitioning airfoils, in which case the only limiting factor is the number of airfoil tables allowed. A second inconvenience is the absence of a variable incidence

stabilator model. This necessitates inefficient "hand" iterations to obtain the correct stabilator incidence angle for the calculated collective pitch angle. A CAMRAD subroutine has been independently developed for this function; however, it was not available for these studies.

An additional drawback of the current CAMRAD analysis is the assumption of linear variation of fuselage lift and moment with angle of attack. For the AH-64A this is sufficient at most reasonable angles of attack, but would cause inaccuracies at greater fuselage pitch attitudes. Perhaps a more significant limitation is in fuselage drag calculation. Although the general drag trend of most fuselage shapes is predicted correctly, the CAMRAD model does not allow for a shift in the drag bucket from zero angle of attack as is the case with the AH-64A.

Main Rotor Natural Frequency Comparisons

The flexibility of the AH-64A hub inboard of the lag hinge has a visible effect on the dynamics characteristics of the rotor. In general, however, the CAMRAD main rotor natural frequency predictions for the AH-64A agree well with the DART results up to eight per revolution.

Main Rotor Blade Structural Loads Comparisons

Before drawing conclusions about the applicability of CAMRAD for AH-64A blade loads predictions, it is important to put the task in the proper perspective. Aeroelastic rotary wing structural loads prediction is a complex problem composed of both aerodynamic and structural modeling challenges. It is well known that the aerodynamic phenomena associated with helicopter main rotors are highly complex and many assumptions must be made in order to predict aerodynamic loads in a reasonably efficient and practical manner. Perhaps more complicated than rotor aerodynamics are rotor structural dynamics. The problem is compounded many-fold when the two facets are combined to give the solution to the blade loads problem.

The advanced rotor system of the AH-64A helicopter is by no means simple. The presence of structural redundancies and advanced geometries is somewhat recent in helicopter rotor system design and analytical techniques have been hard pressed to keep pace. It is recognized that highly flexible structural analysis models are needed to accurately represent these unconventional systems.

In light of these general observations, the blade structural loads correlation results presented in the previous section are summarized below.

1. Flapwise bending moments are well predicted by CAMRAD and DART. There is some concern about the CAMRAD calculation of bending loads from stiffness and curvature at the blade root due to the rapid rate of change in flapwise stiffness in that region.

2. Chordwise bending moments are better predicted by CAMRAD than by DART. However, the level of correlation with test data is not entirely acceptable. Drive train dynamics are thought to be a contributor to the poor cyclic load correlation.

3. Steady nose-down torsion is overpredicted by both analyses. Cyclic torsion correlation with test measurements is also poor for both CAMRAD and DART. It is conceivable that the inaccurate elastic axis modeling in CAMRAD has a negative effect on the results.

4. It has been demonstrated using other analyses that the location of the elastic axis has an impact on blade structural loads prediction. However, the effects were found to be somewhat analysis dependent and relatively insignificant in light of the generally poor level of correlation with test data.

5. The inclusion of additional torsion degrees of freedom over and above the two modes utilized for the baseline loads predictions had essentially no effect on the structural loads predictions. Inclusion of an additional 4 bending modes had a significant impact on the steady chordwise loads. Trim and performance predictions were uneffected by the additional modes.

Summary

The comprehensive nature of the CAMRAD analysis program is a very important attribute for the multidisciplinary task of aeroelastic loads prediction. Some limitations in the analytical methods employed in the code have been pointed out in the preceding pages. However, in spite of these restrictions, the general indication is that the effects are relatively insignificant in light of more fundamental problems associated with the analytical modeling of the complex phenomena which make up the helicopter structural dynamics problem. This problem, as associated with the AH-64A in particular, appears to be solved as well, or in some cases better, by CAMRAD as by the more detailed model available in DART. However, as rotor systems continue to become more structurally and geometrically complex, it is anticipated that the distinction between the analyses will become more definite.

RECOMMENDATIONS

The scope of the present study as well as limitations in test data available did not allow for a complete evaluation of the CAMRAD AH-64A model. Additional studies are expected to produce some improvement in performance and rotor blade loads predictions. Such studies would involve airloads comparisons including exploration of the various wake and unsteady aerodynamics models available, in addition to further investigation into the structural modeling options, such as the inclusion of drive train effects. The comparisons with flight test data performed here are by no means complete. Additional test data is needed in order to draw more definite conclusions as to the accuracy of the predictions.

An additional effort of interest would involve modification of the CAMRAD code to accept blade mode shapes as input. This would bypass the use in CAMRAD of mode shapes based on the limited number of blade root configurations and would thus eliminate one area of the modeling inaccuracy. This approach could also be taken for modeling bearingless rotors. However, it is not anticipated that it will offer a CAMRAD model suitable for bearingless rotor modeling.

REFERENCES

1. Johnson, W., "A Comprehensive Analytical Model of Rotorcraft Aerodynamics and Dynamics, Part I: Analysis Development," NASA TM 81182, 1980.

2. Johnson, W., "A Comprehensive Analytical Model of Rotorcraft Aerodynamics and Dynamics, Part II: User's Manual," NASA TM 81183, 1980.

3. Johnson, W., "A Comprehensive Analytical Model of Rotorcraft Aerodynamics and Dynamics, Part III: Program Manual," NASA TM 81184, 1980.

4. Harrison, J. M., "An Integrated Approach to Effective Analytical Support of Helicopter Design and Development," Paper presented at the Sixth European Rotorcraft and Powered Lift Aircraft Forum, Bristol, England, September 1980.

5. Sadler, S.G., "Development and Application of a Method for Predicting Rotor Free Wake Positions and Resulting Rotor Blade Airloads." NASA CR 1911 and CR 1912, December 1971.

6. Kocurek, J. D., Berkowitz, L. F., Harris, F. D., "Hover Performance Methodology at Bell Helicopter Textron," presented at the 36th Annual Forum of the AHS, Washington, D.C., May 1980.

7. Peterson, L., "SADSAM User's Manual," and "Theoretical Basis for SADSAM Computer Program," MSR-10, The MacNeal-Schwendler Corporation, December 1970.

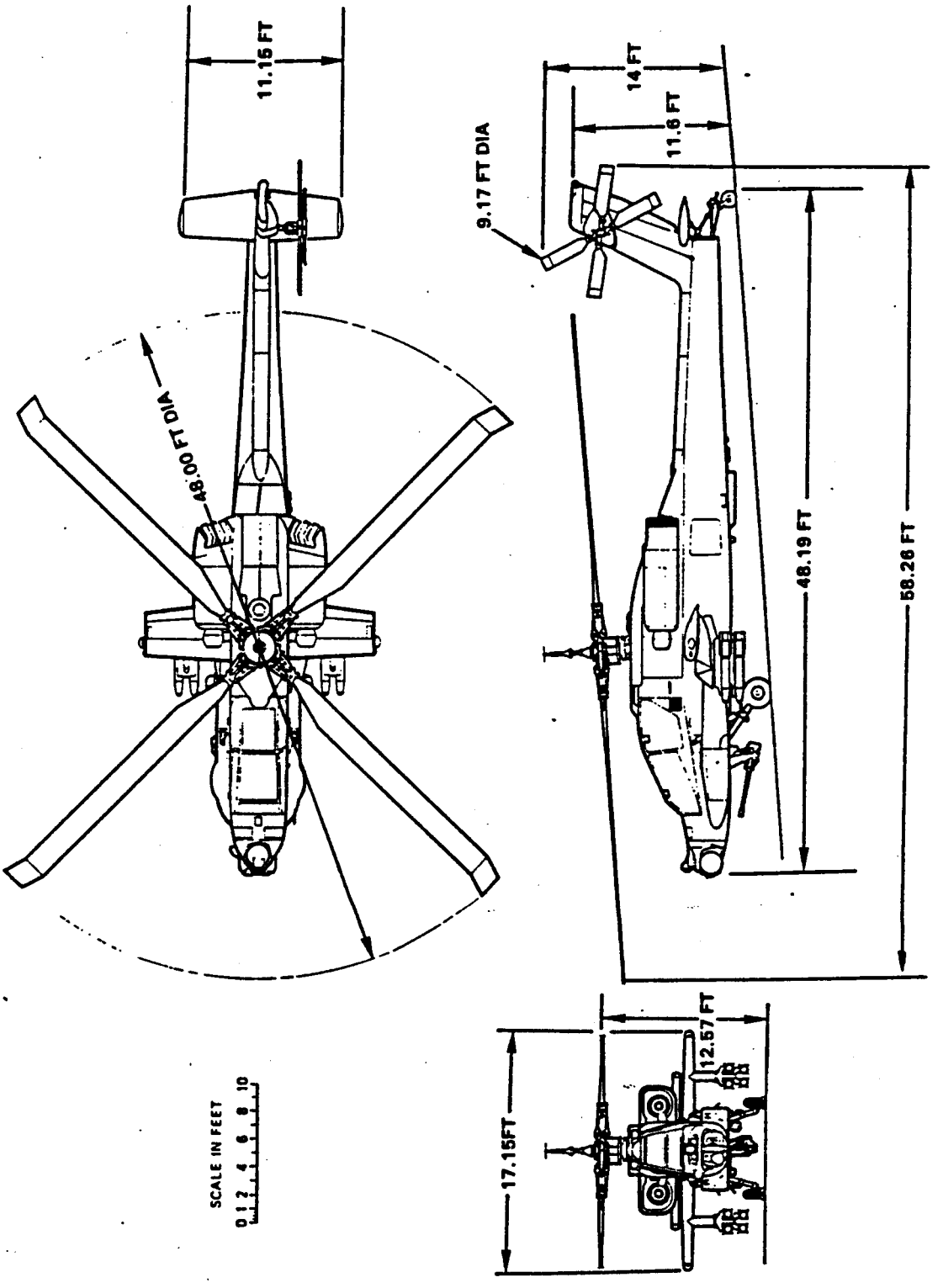

Figure 1. McDonnell Douglas AH-64A Helicopter

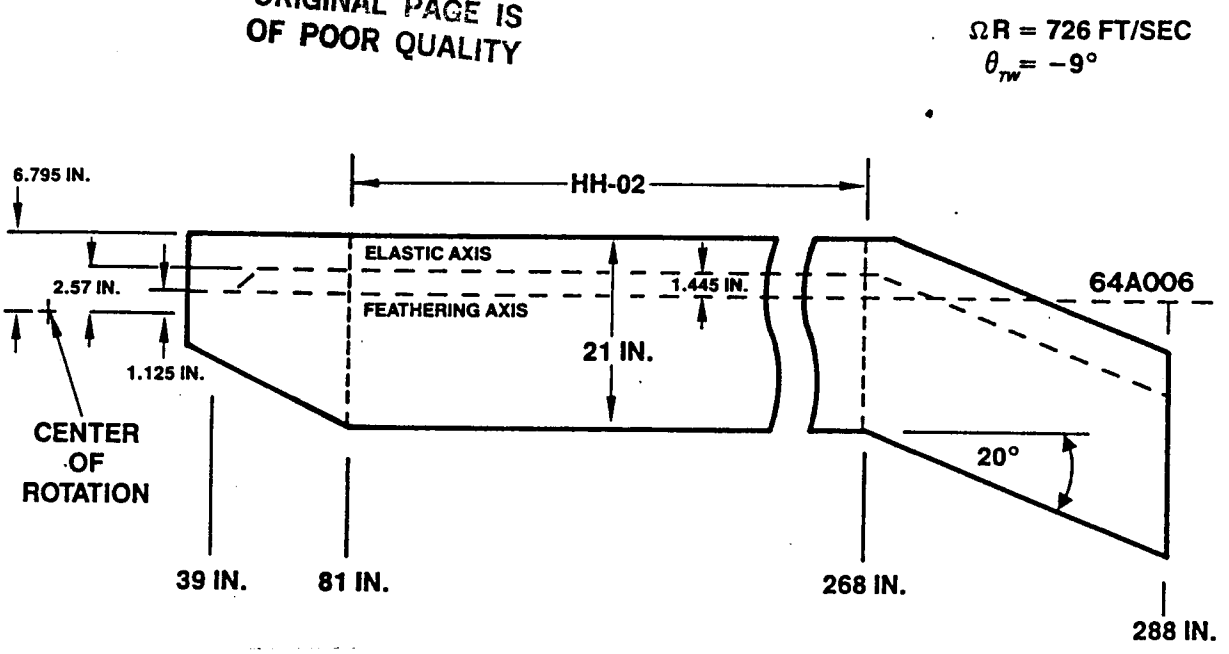

Figure 2. AH-64A Main Rotor Blade

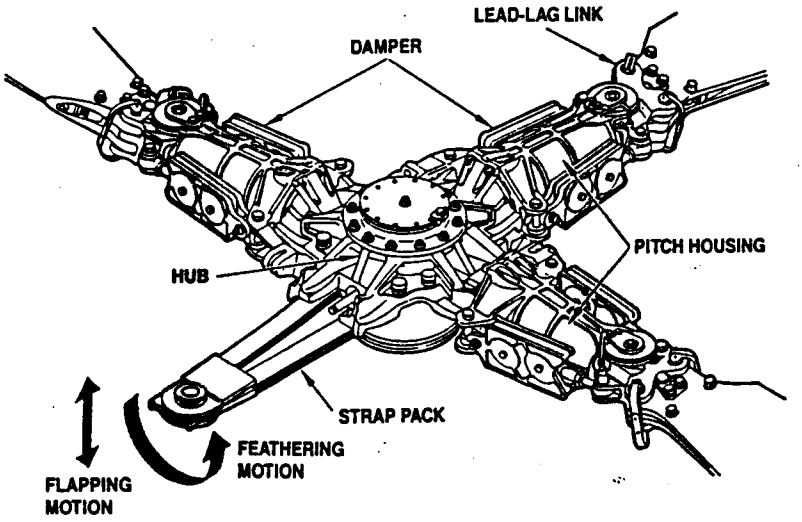

Figure 3. AH-64A Main Rotor Hub

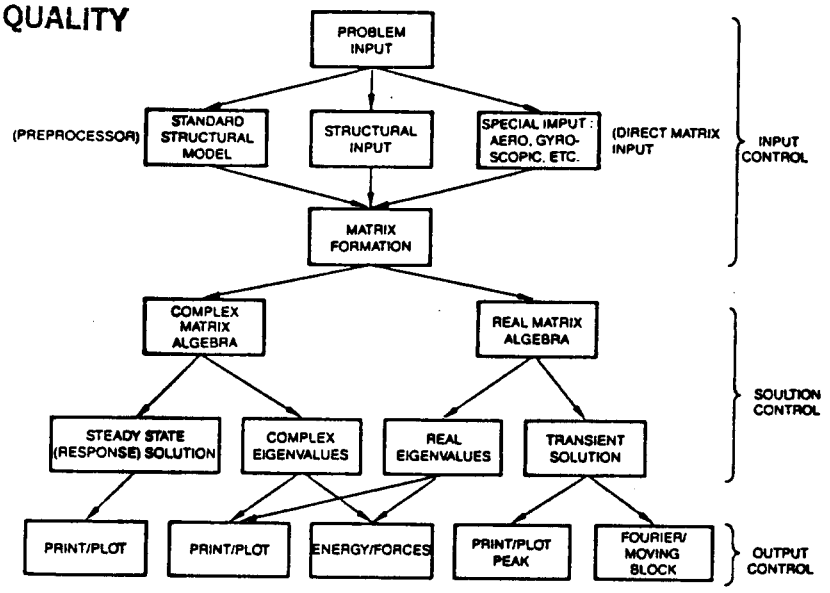

Figure 4. DART - General Description

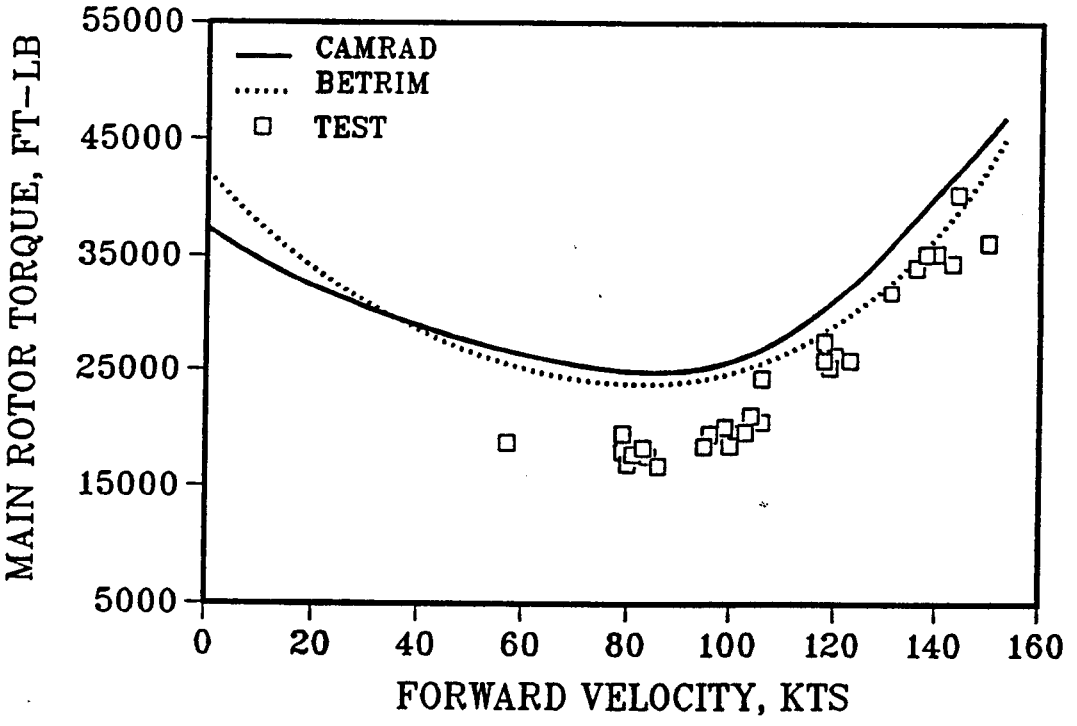

Figure 5. Main Rotor Torque vs. Flight Speed

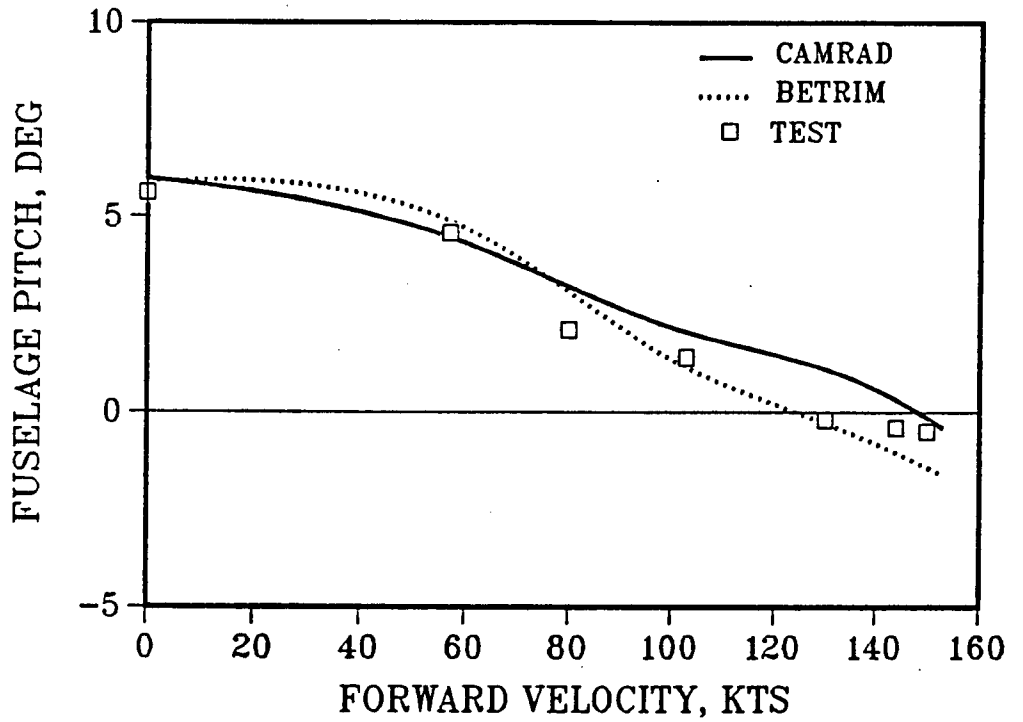

Figure 6a. Fuselage Pitch Attitude vs. Flight Speed

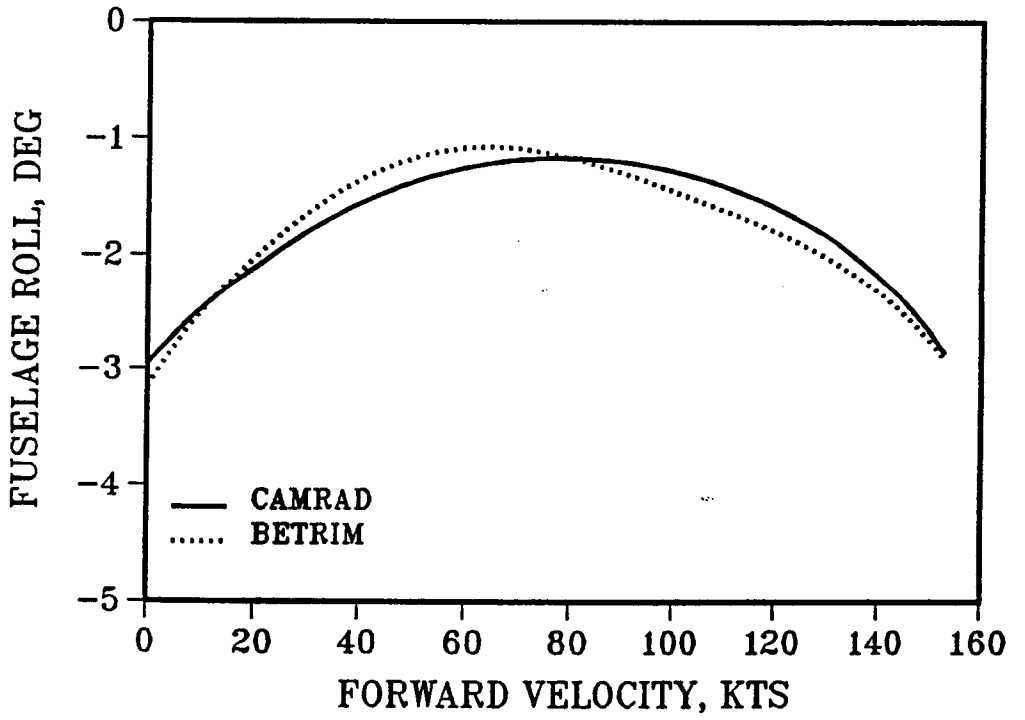

Figure 6b. Fuselage Roll Attitude vs. Flight Speed

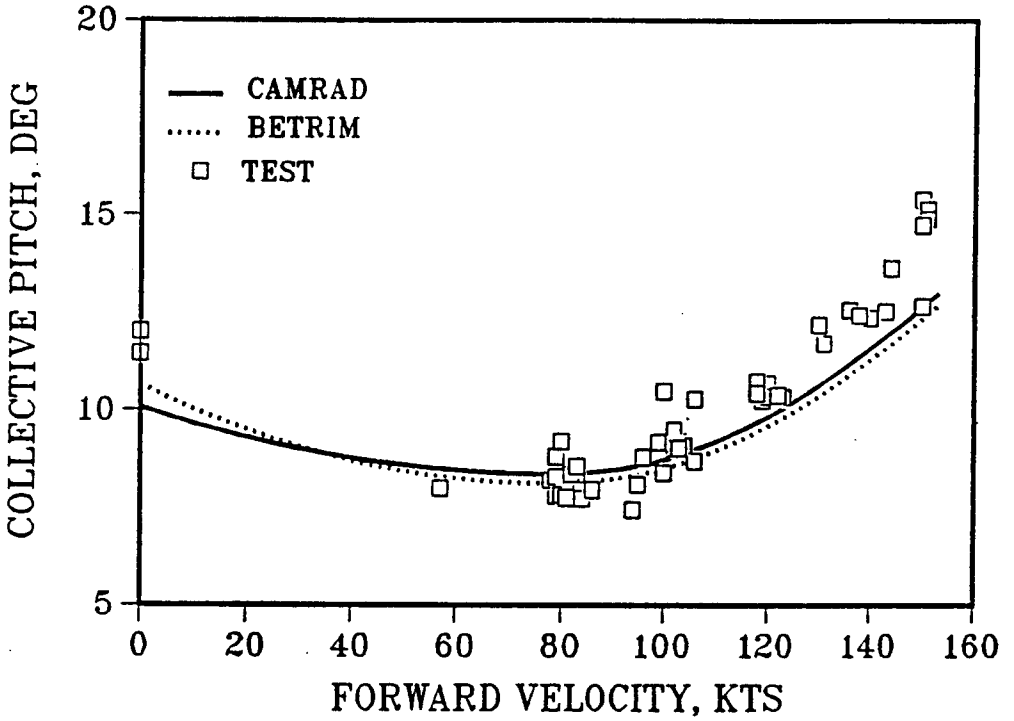

Figure 7. Main Rotor Collective Pitch vs. Flight Speed

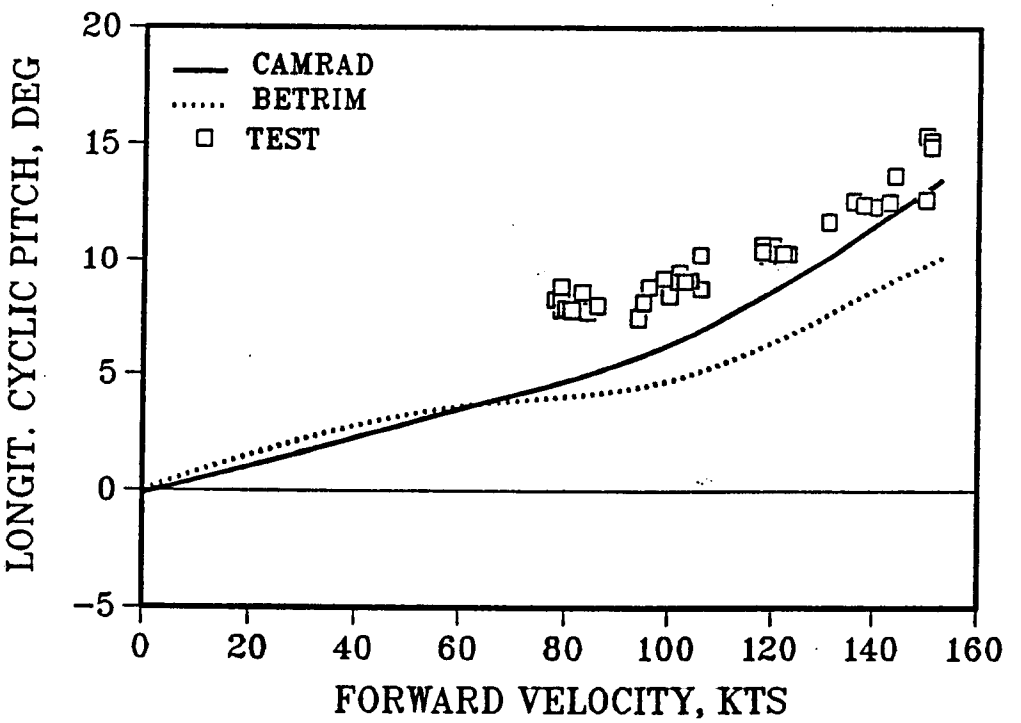

Figure 8. Main Rotor Longit. Cyclic Pitch vs. Flight Speed

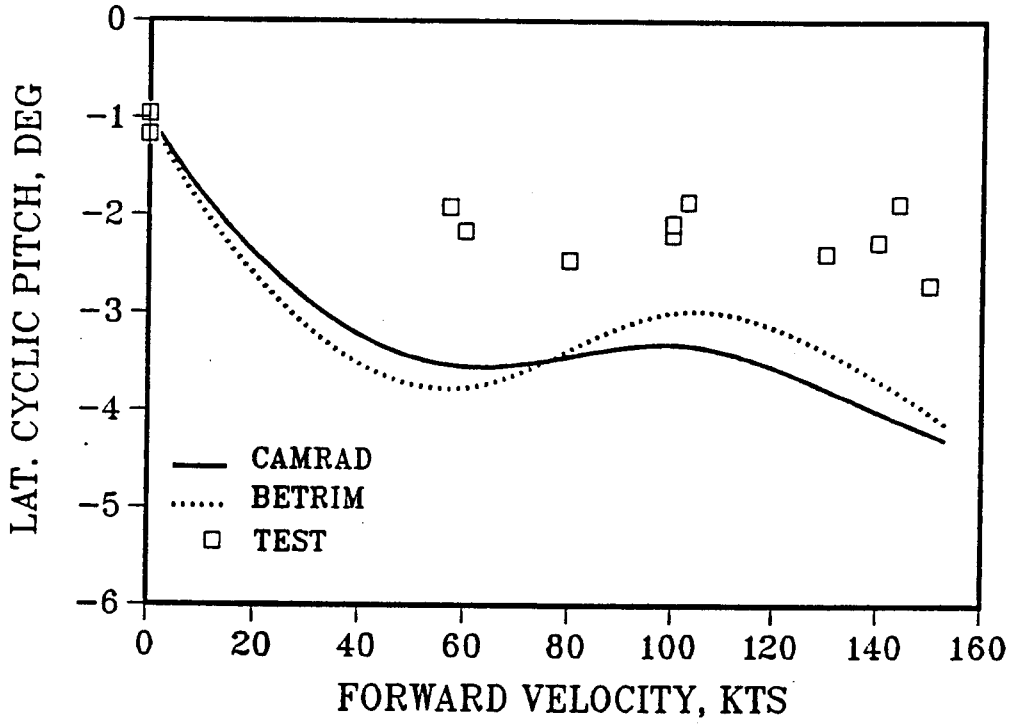

Figure 9. Main Rotor Lat. Cyclic Pitch vs. Flight Speed

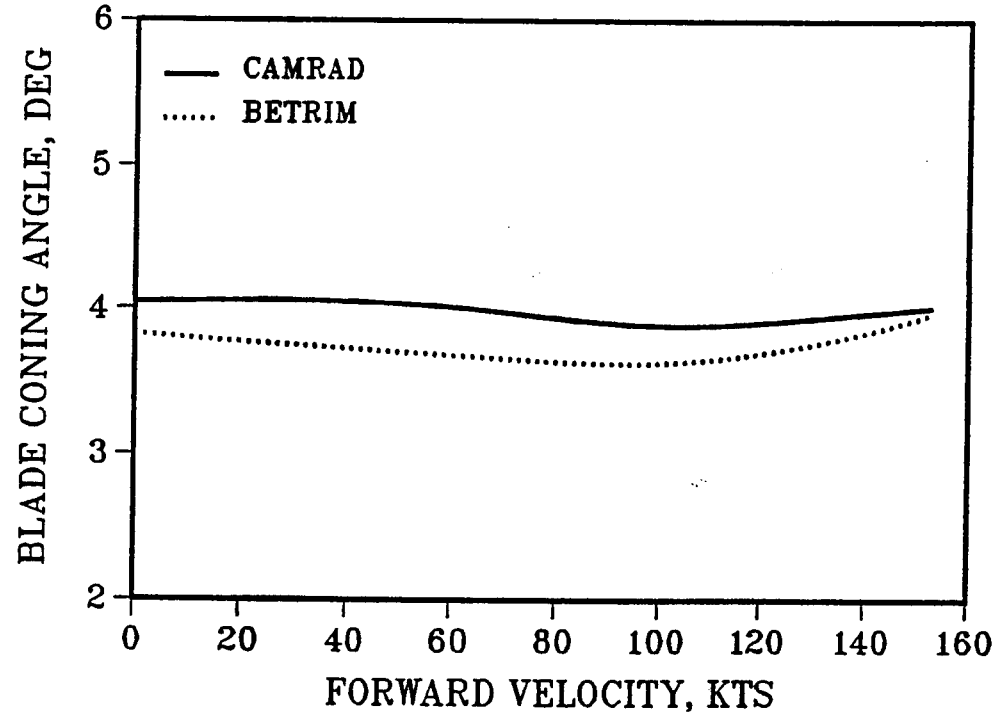

Figure 10. Main Rotor Coning Angle vs. Flight Speed

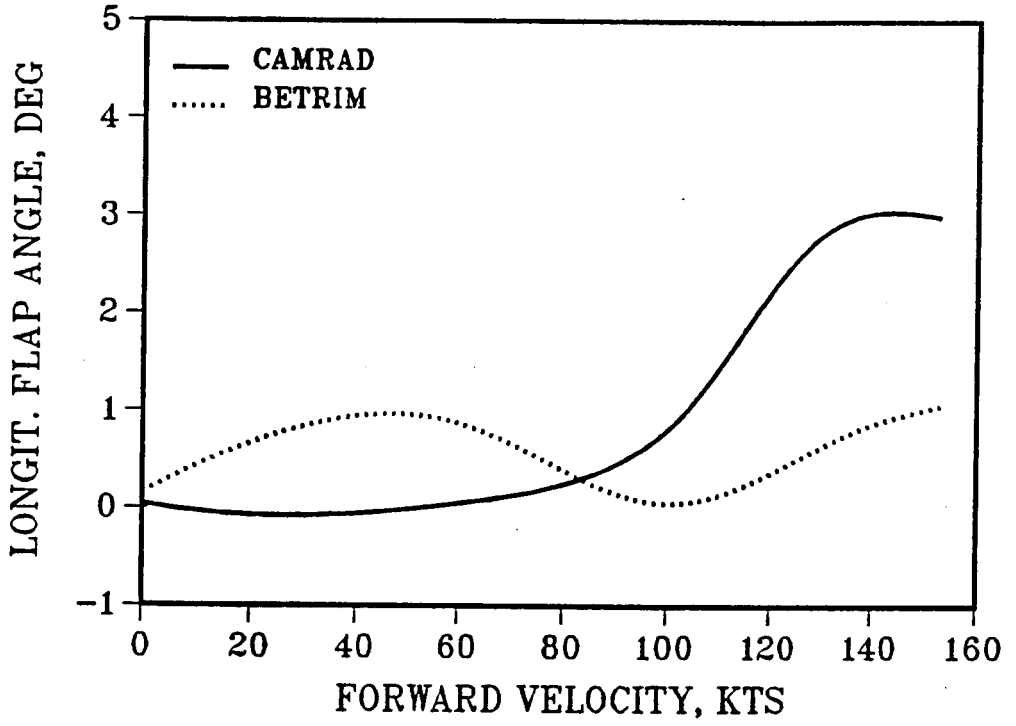

Figure 11. Main Rotor Longit. Flap Angle vs. Flight Speed

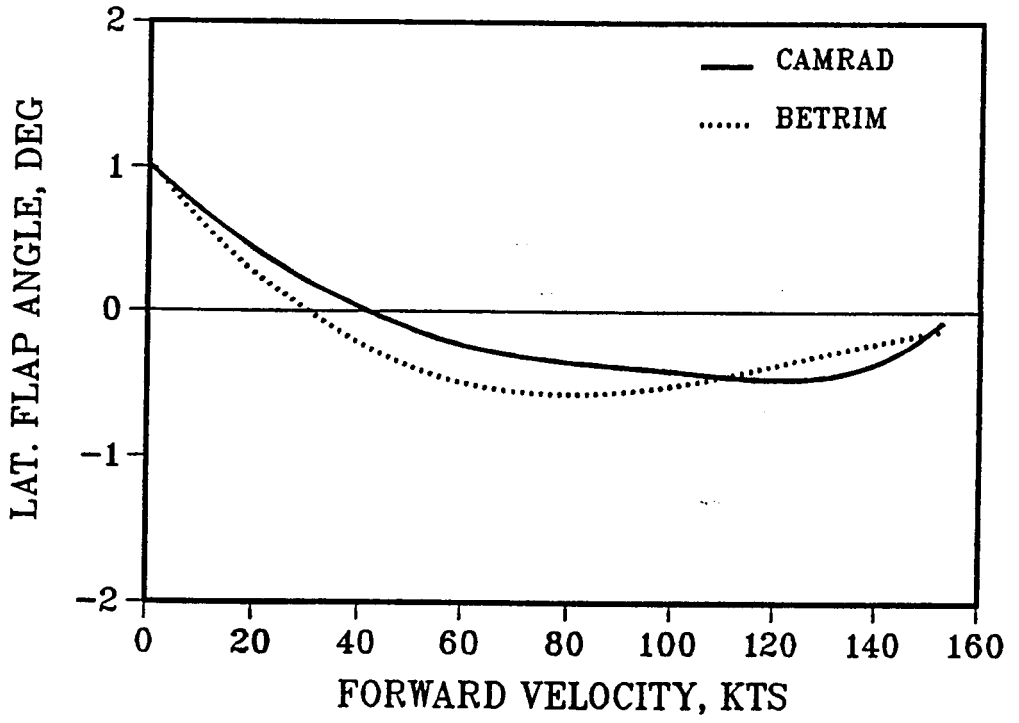

Figure 12. Main Rotor Lat. Flap Angle vs. Flight Speed

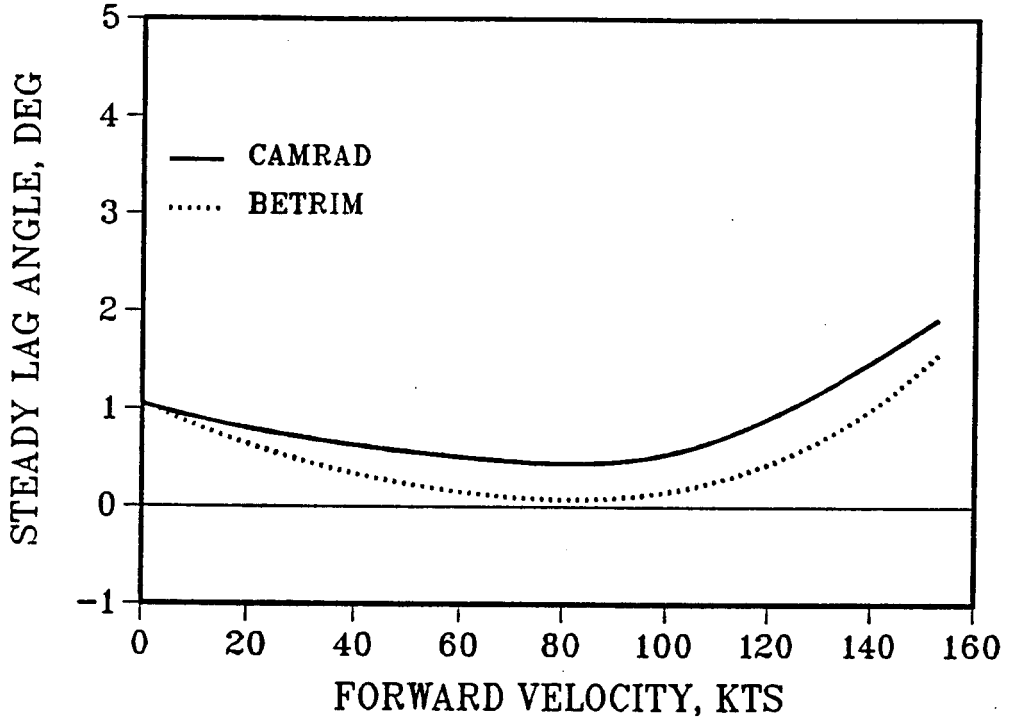

Figure 13. Steady Lag Angle vs. Flight Speed

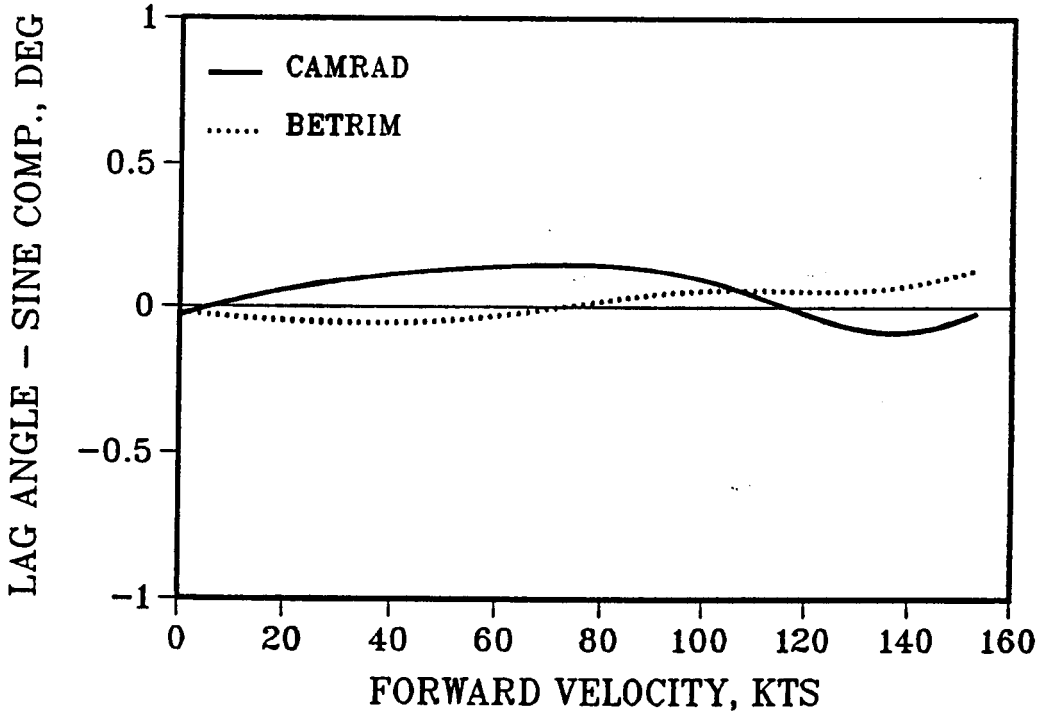

Figure 14. Lag Angle, Sine Component vs. Flight Speed

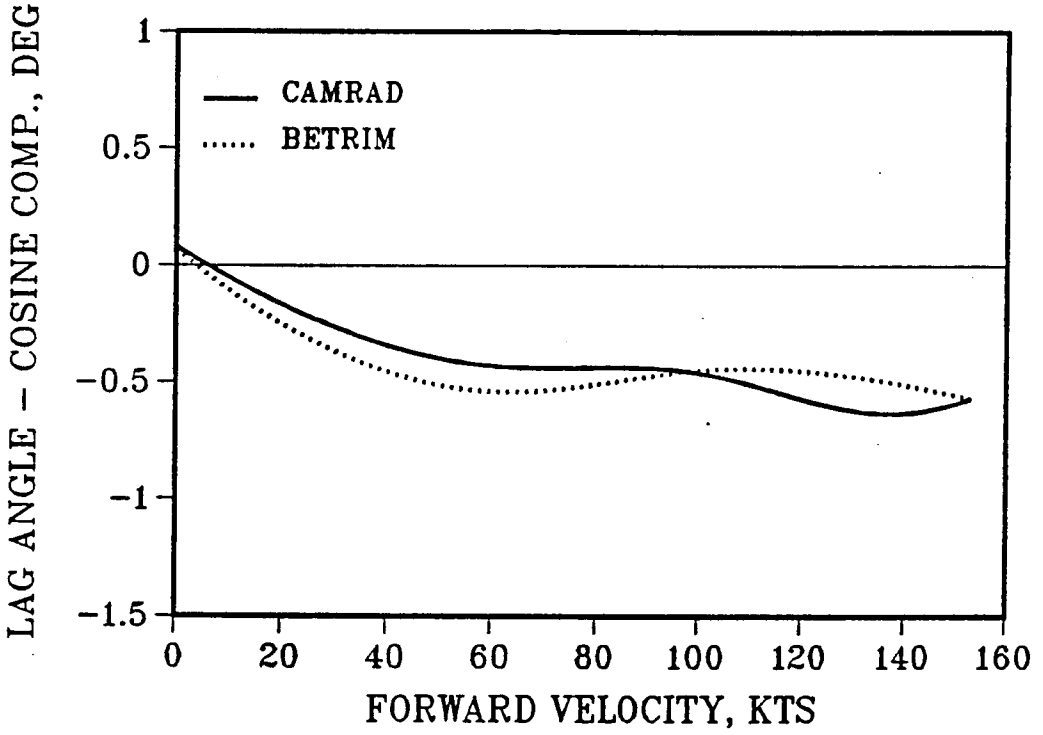

Figure 15. Lag Angle, Cosine Component vs. Flight Speed

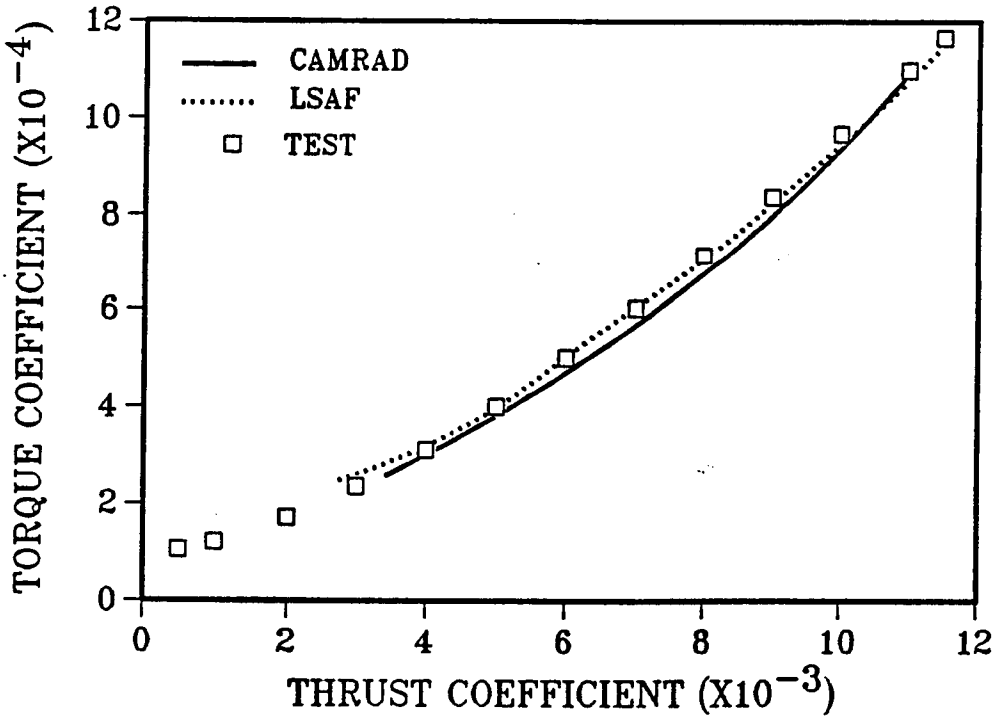

Figure 16. Hover Performance

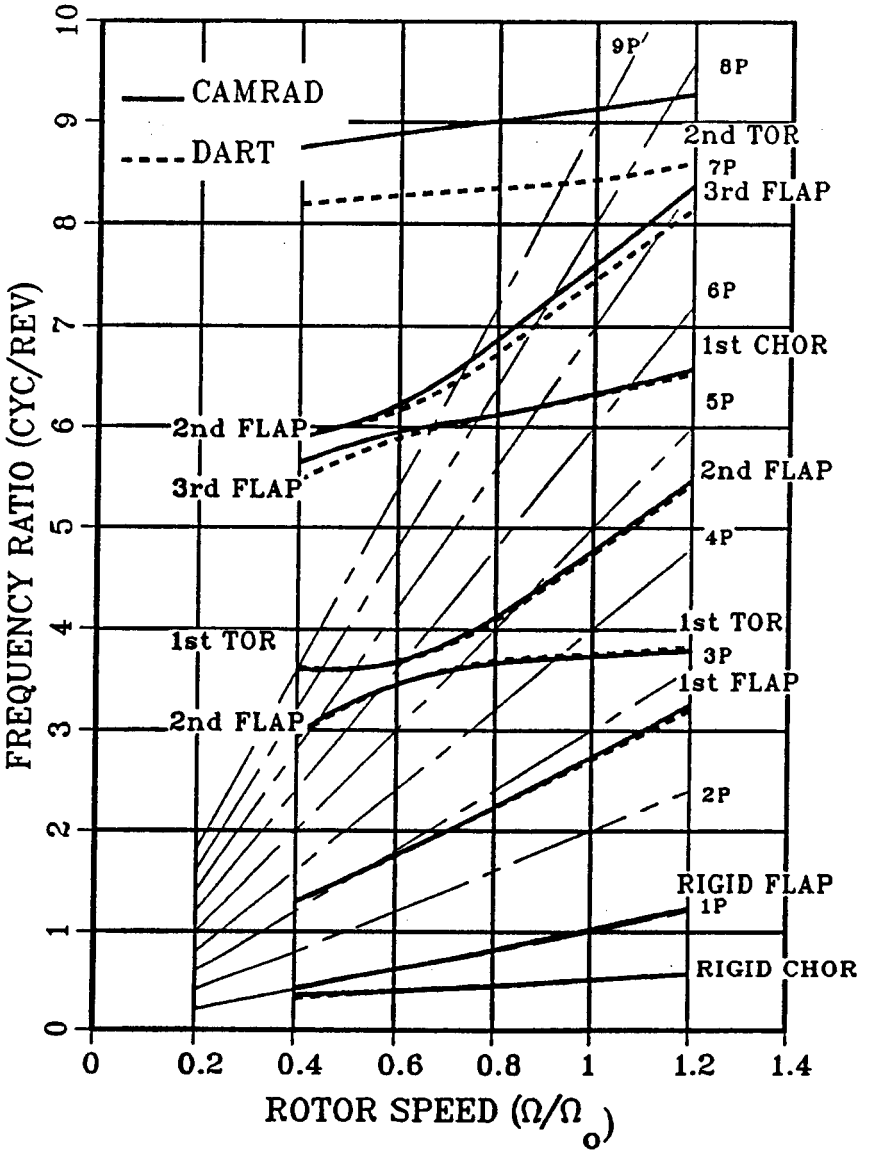

Figure 17. AH–64A Main Rotor Resonances – Cyclic Modes in vacuo

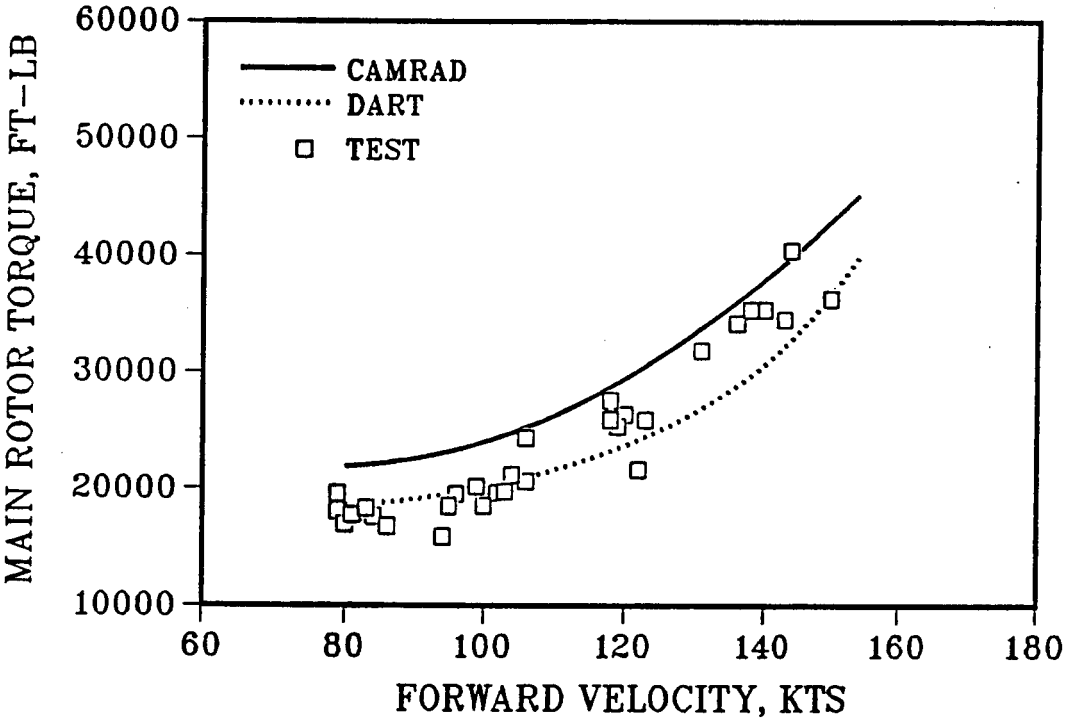

Figure 18. Main Rotor Torque vs. Flight Speed

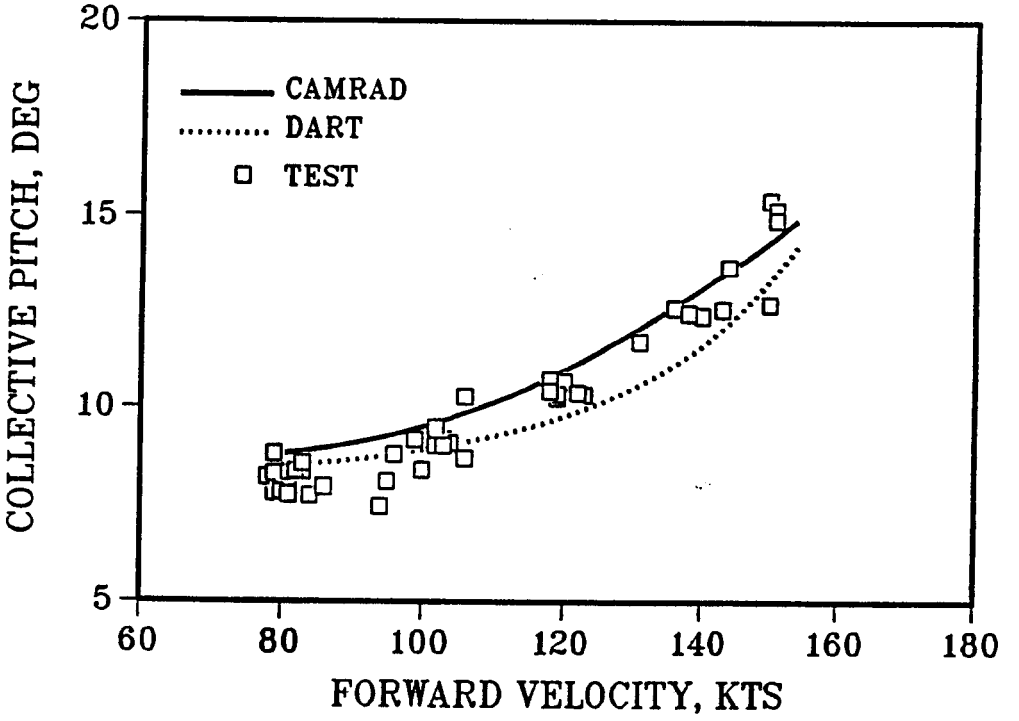

Figure 19. Main Rotor Collective Pitch vs. Flight Speed

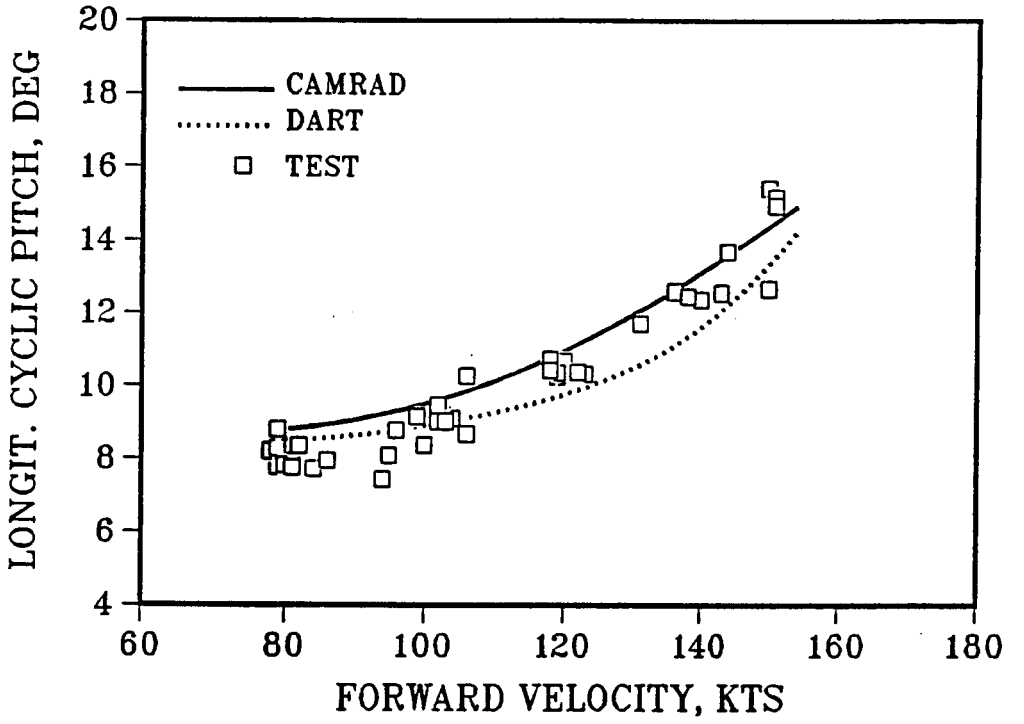

Figure 20. Main Rotor Longit. Cyclic Pitch vs. Flight Speed

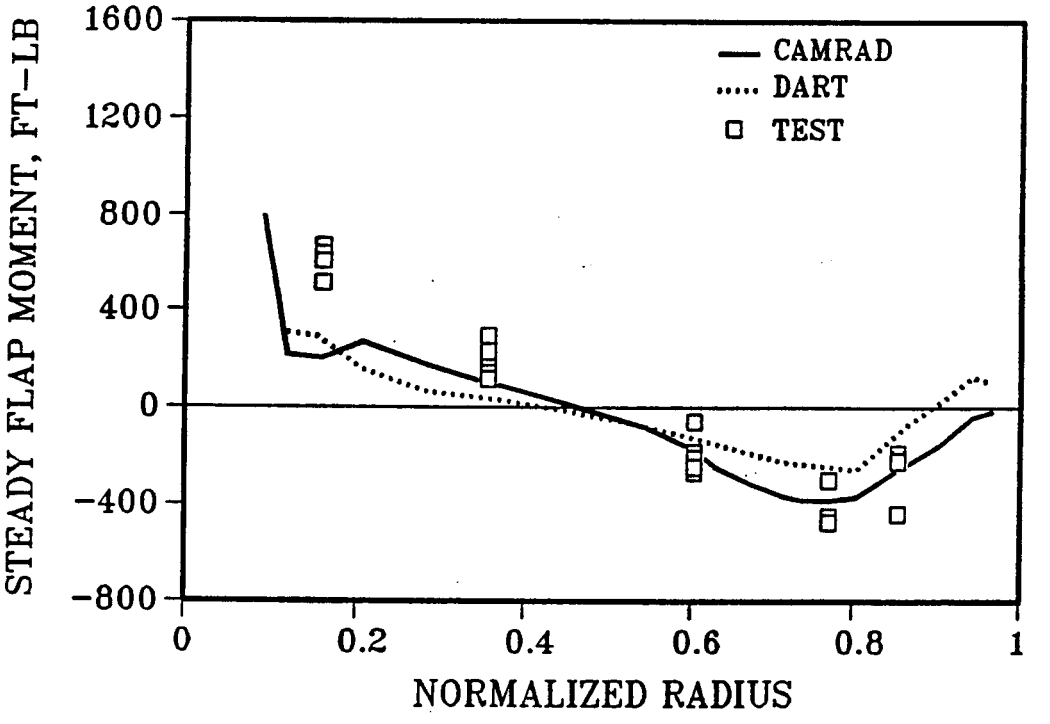

Figure 21a. Steady Flap Bending Moment vs. Radius – 100 kts.

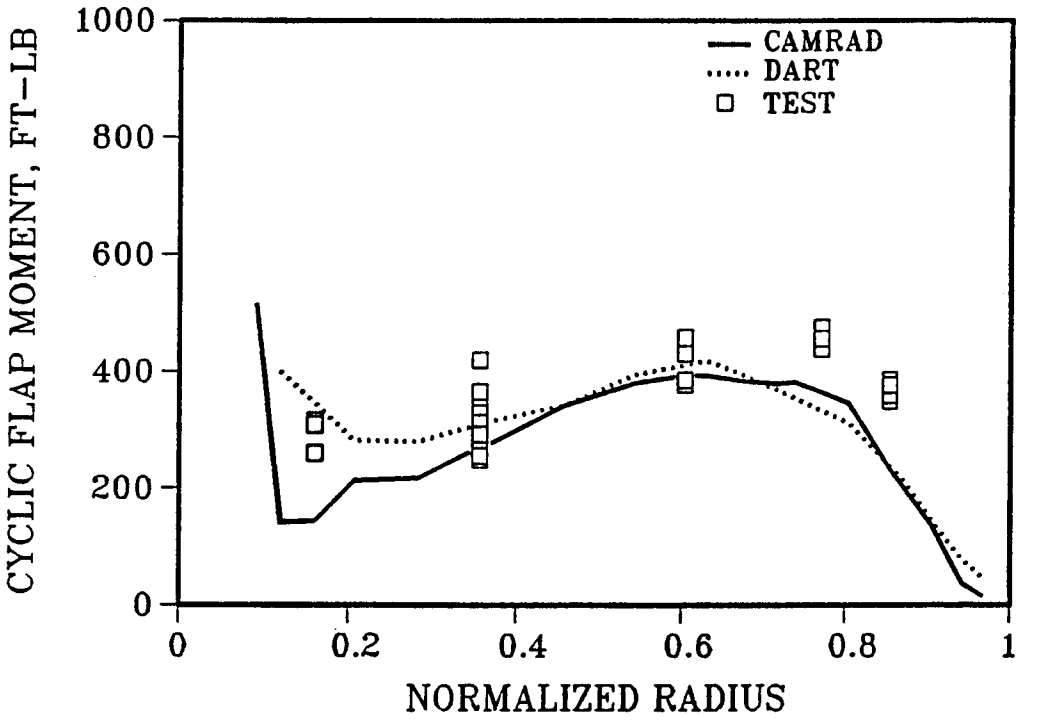

Figure 21b. Cyclic Flap Bending Moment vs. Radius – 100 kts.

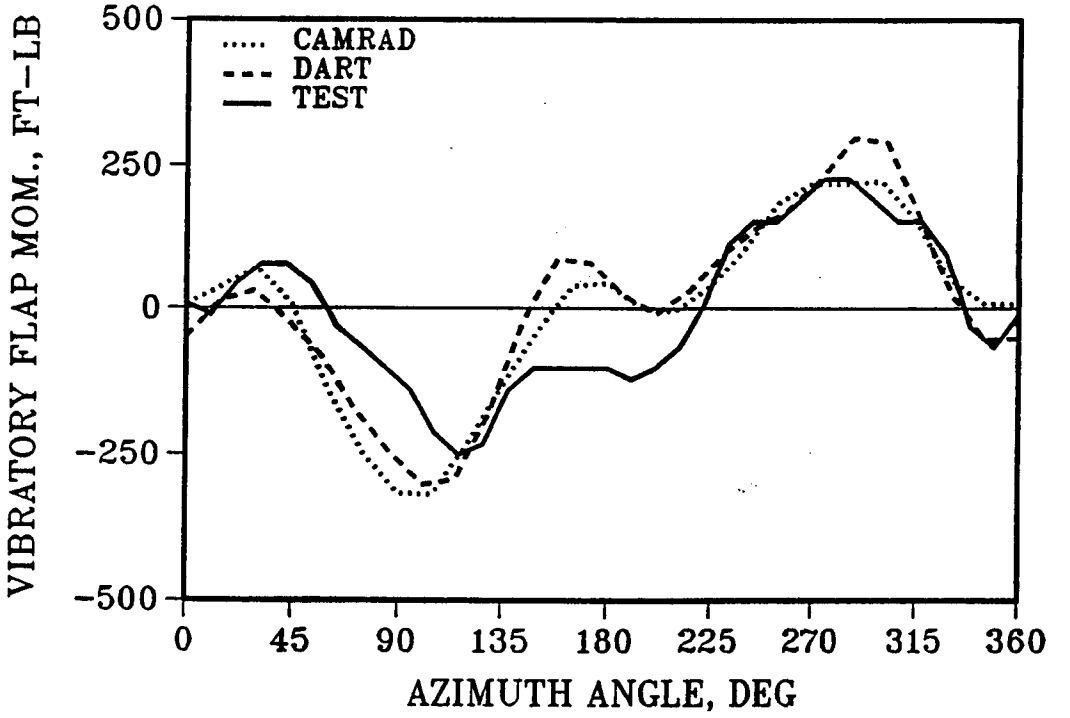

Figure 22. Flap Bending Time History at .36R – 100 kts.

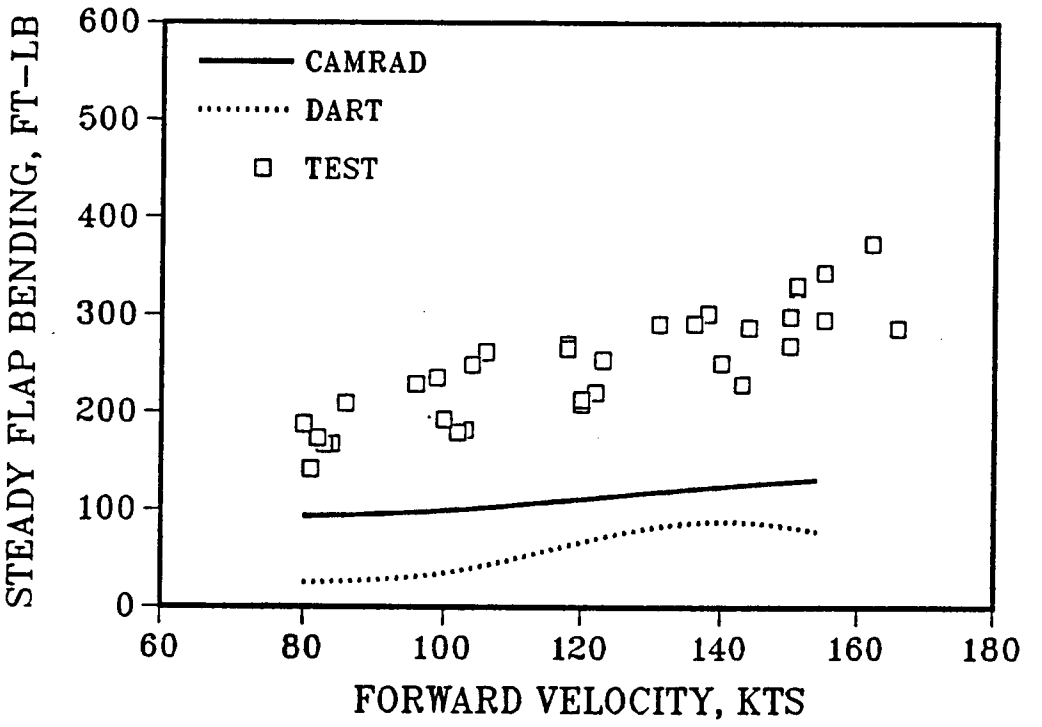

Figure 23a. Steady Flap Bending at .36R vs. Flight Speed

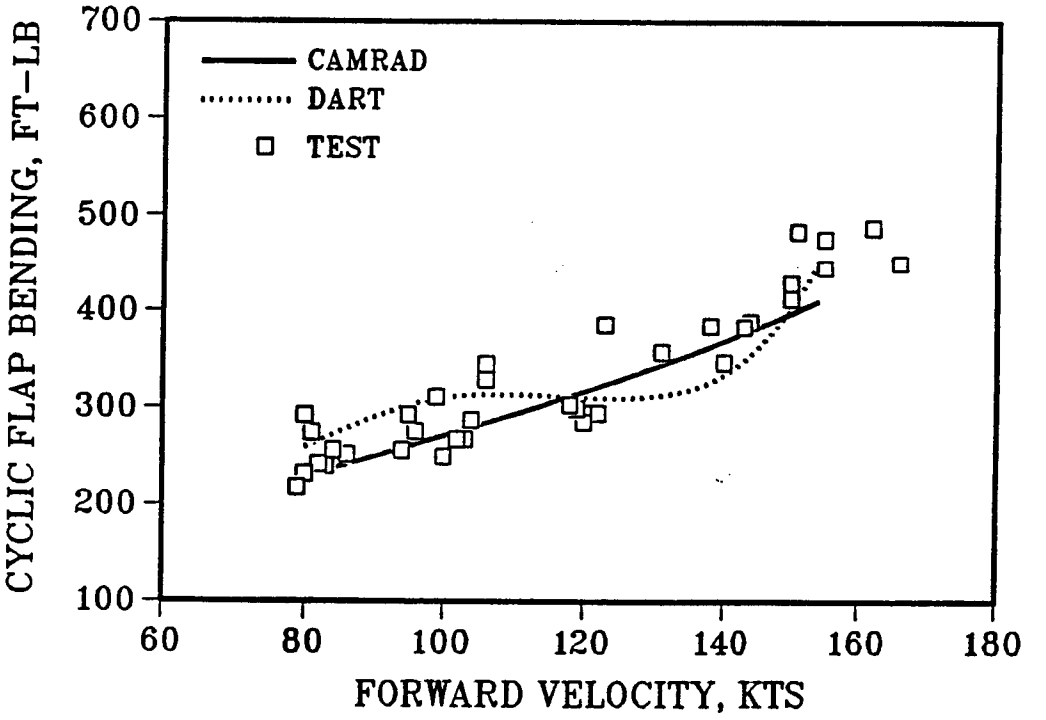

Figure 23b. Cyclic Flap Bending at .36R vs. Flight Speed

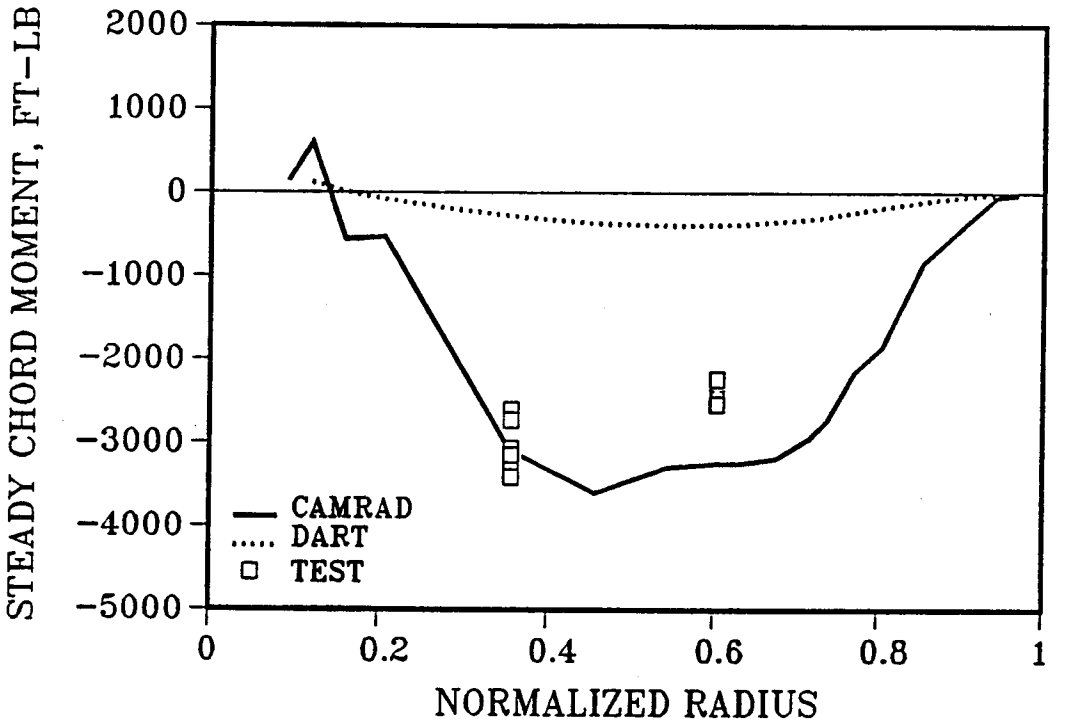

Figure 24a. Steady Chord Bending Moment vs. Radius – 100 kts.

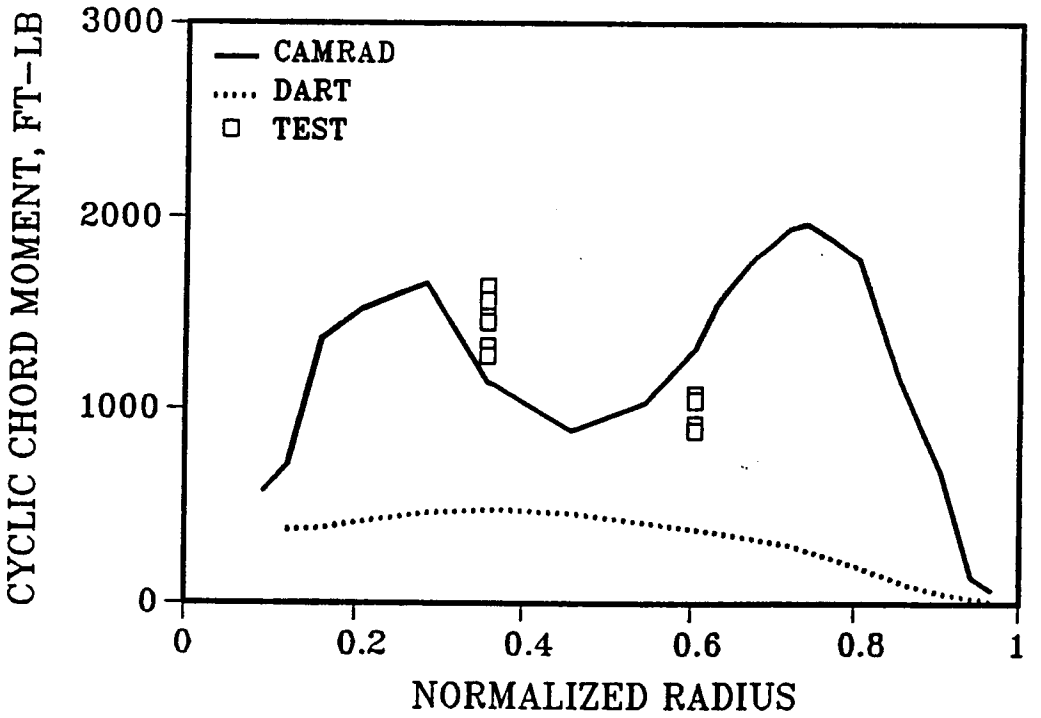

Figure 24b. Cyclic Chord Bending Moment vs. Radius – 100 kts.

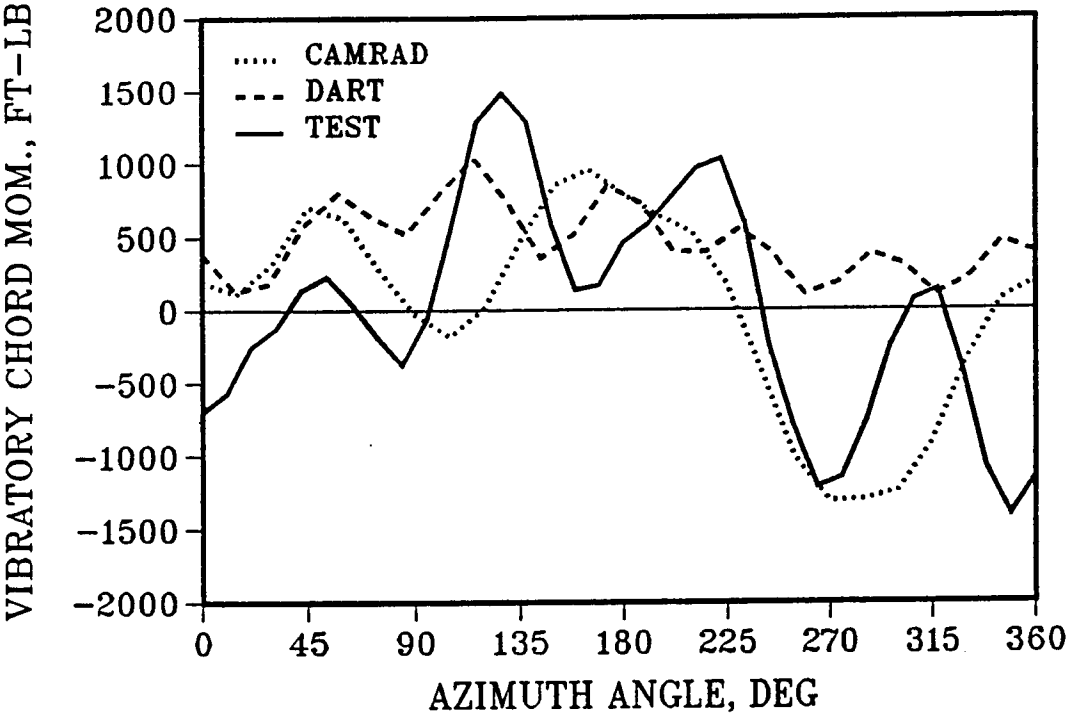

Figure 25. Chord Bending Time History at .36R – 100 kts.

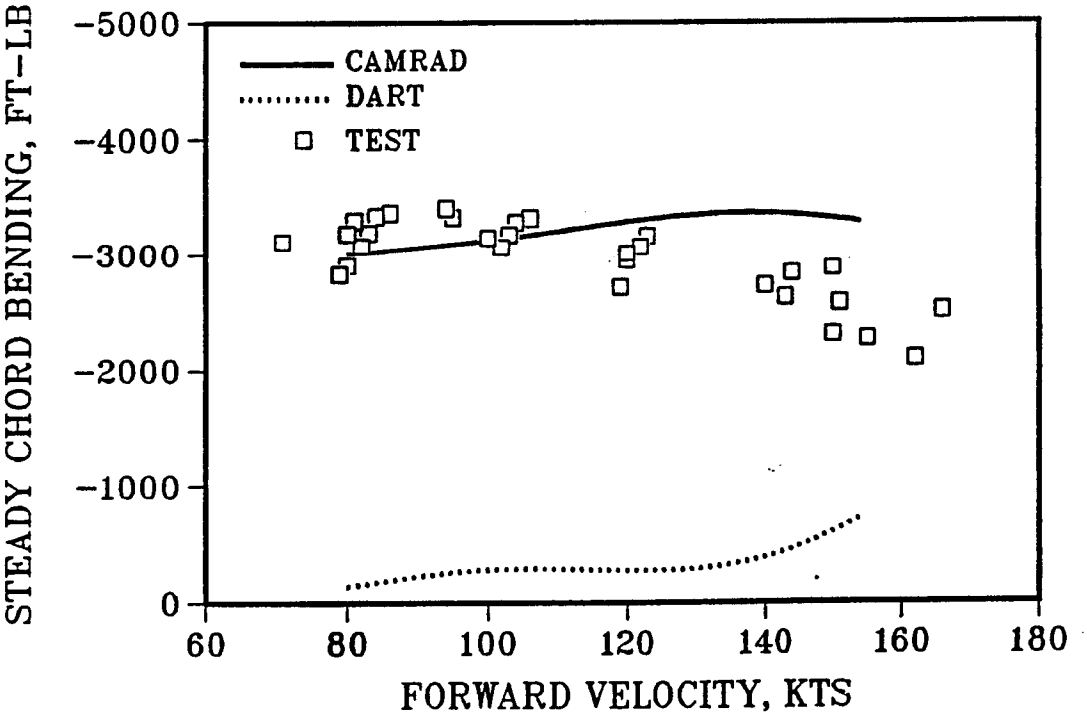

Figure 26a. Steady Chord Bending at .36R vs. Flight Speed

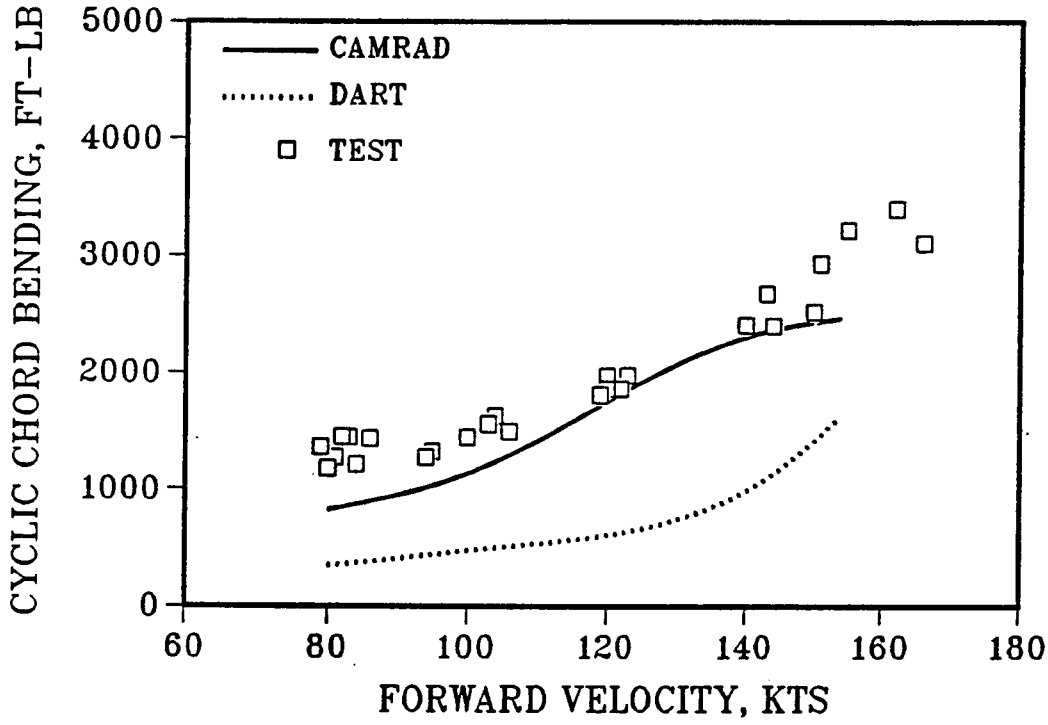

Figure 26b. Cyclic Chord Bending at .36R vs. Flight Speed

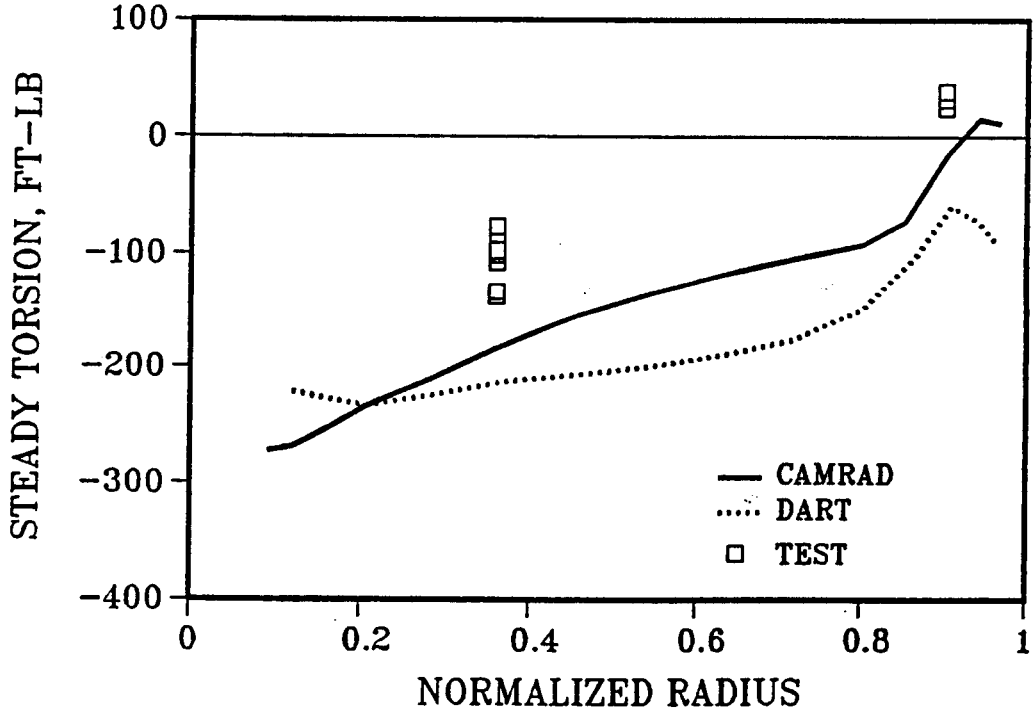

Figure 27a. Steady Torsion Moment vs. Radius – 100 kts.

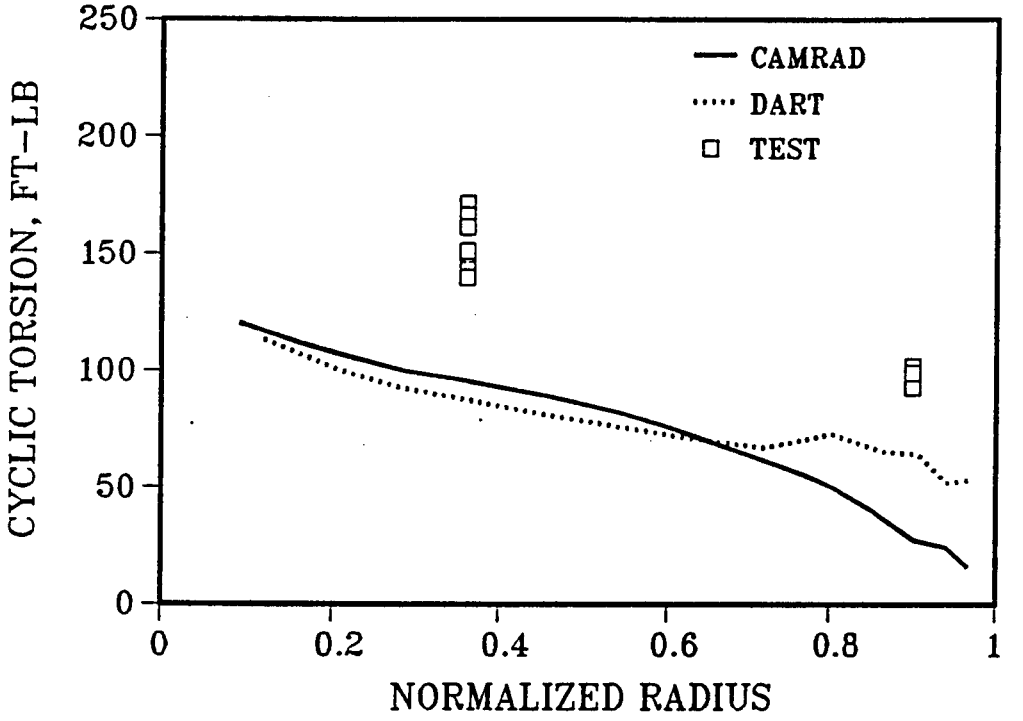

Figure 27b. Cyclic Torsion Moment vs. Radius – 100 kts.

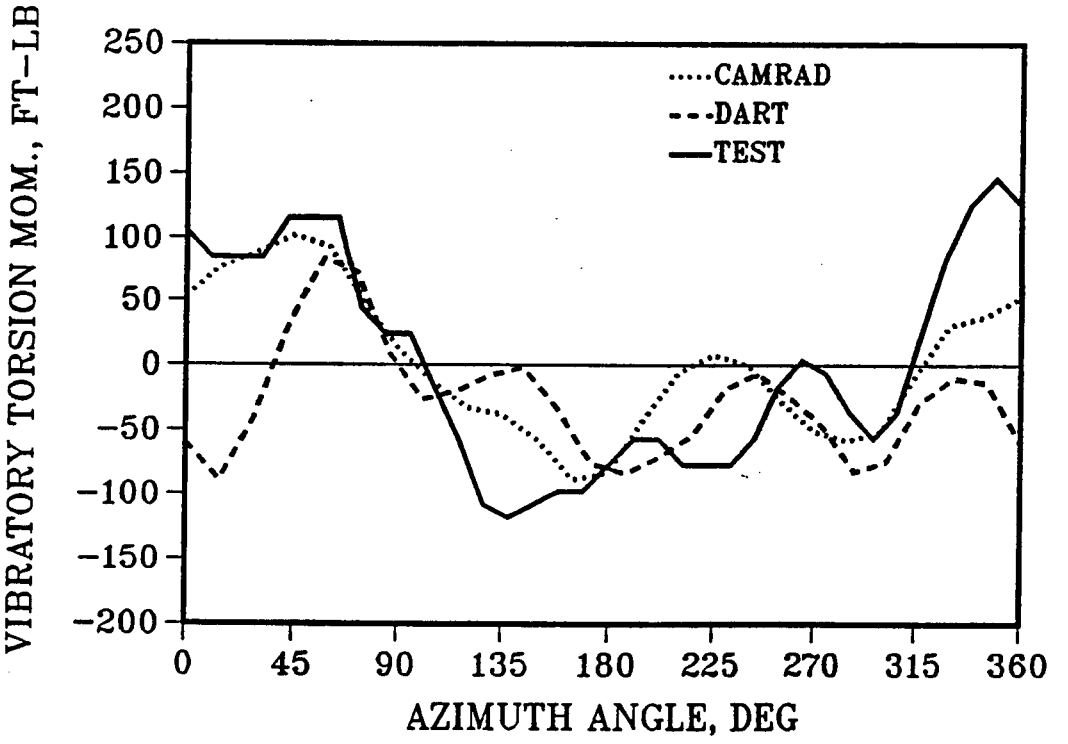

Figure 28. Torsion Time History at .36R – 100 kts.

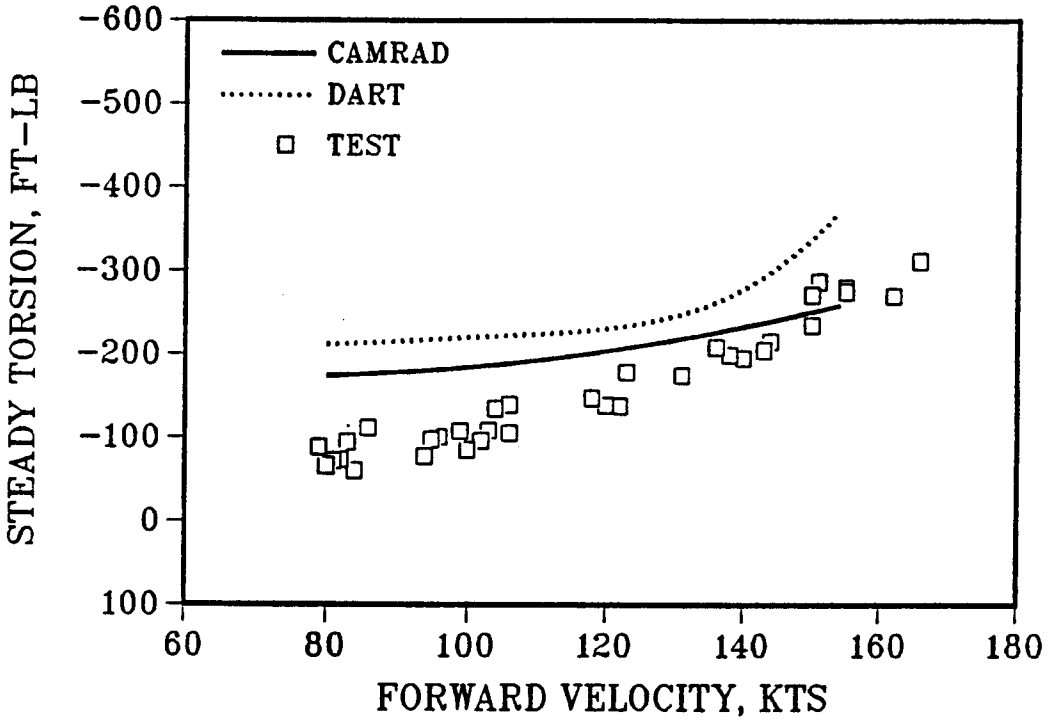

Figure 29a. Steady Torsion at .36R vs. Flight Speed

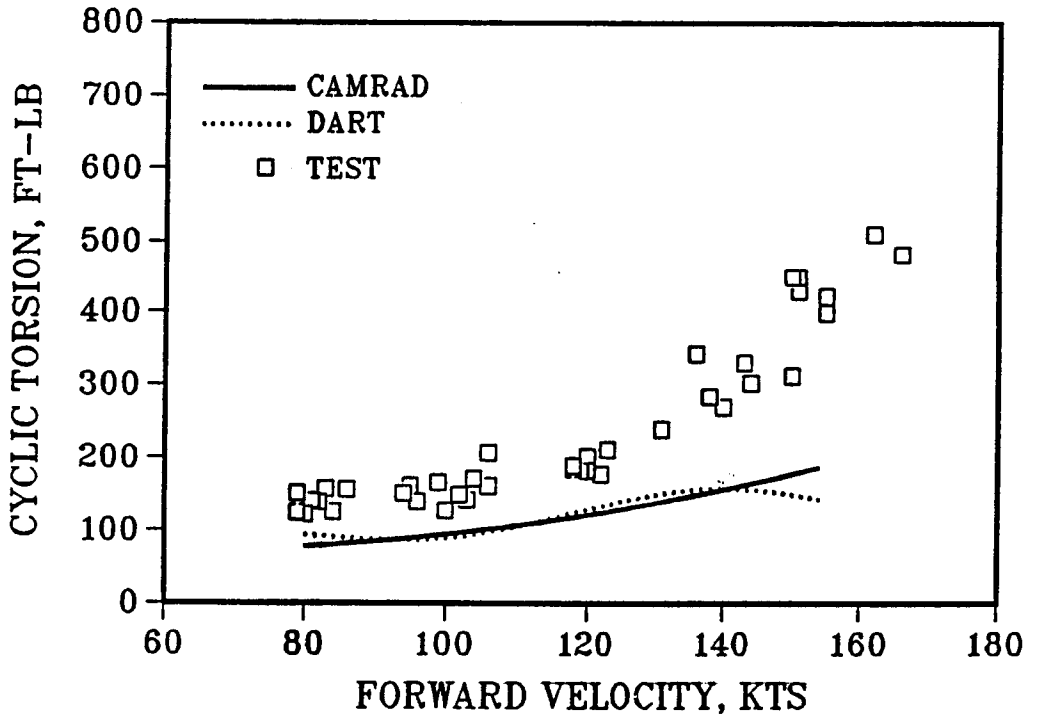

Figure 29b. Cyclic Torsion at .36R vs. Flight Speed

APPENDIX A:

ADDITIONAL STRUCTURAL LOADS COMPARISONS

CAMRAD, DART and flight test measured loads comparisons are presented in the following pages in figures A-1 to A-18 for the 80, 140, and 154 knots level flight conditions and hover out of ground effect. The plots are in the forms of steady and cyclic bending moment versus radial station and time histories of vibratory bending moment at 36 percent radius. Time histories are not shown for the hover condition.

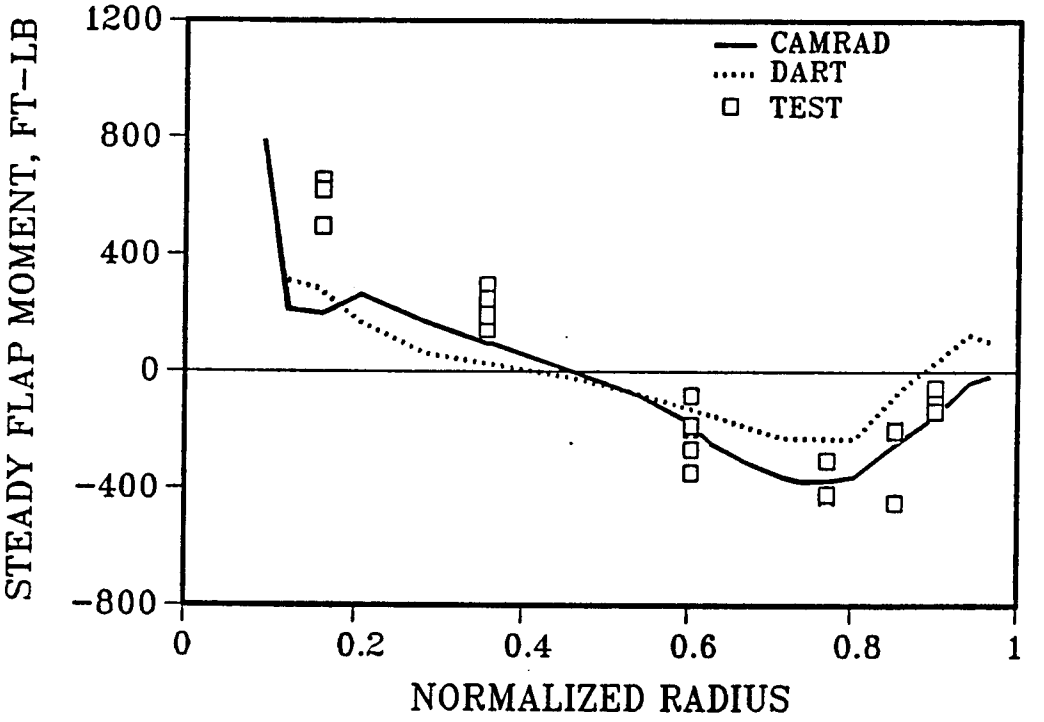

Figure A–1a. Steady Flap Bending Moment vs. Radius – 80 kts.

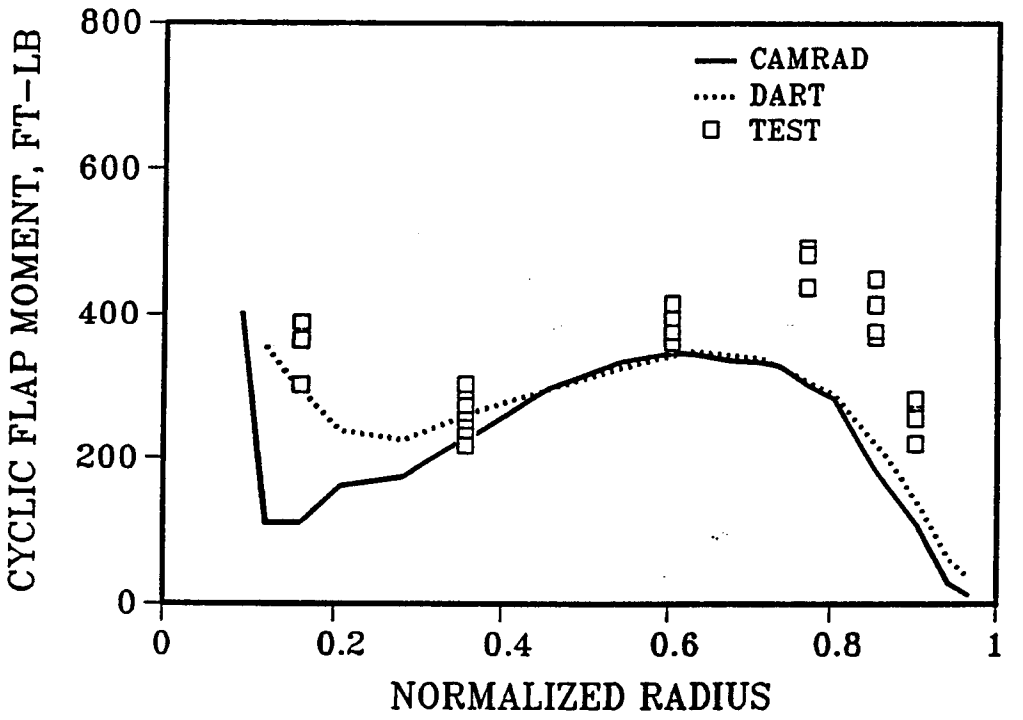

Figure A–1b. Cyclic Flap Bending Moment vs. Radius – 80 kts.

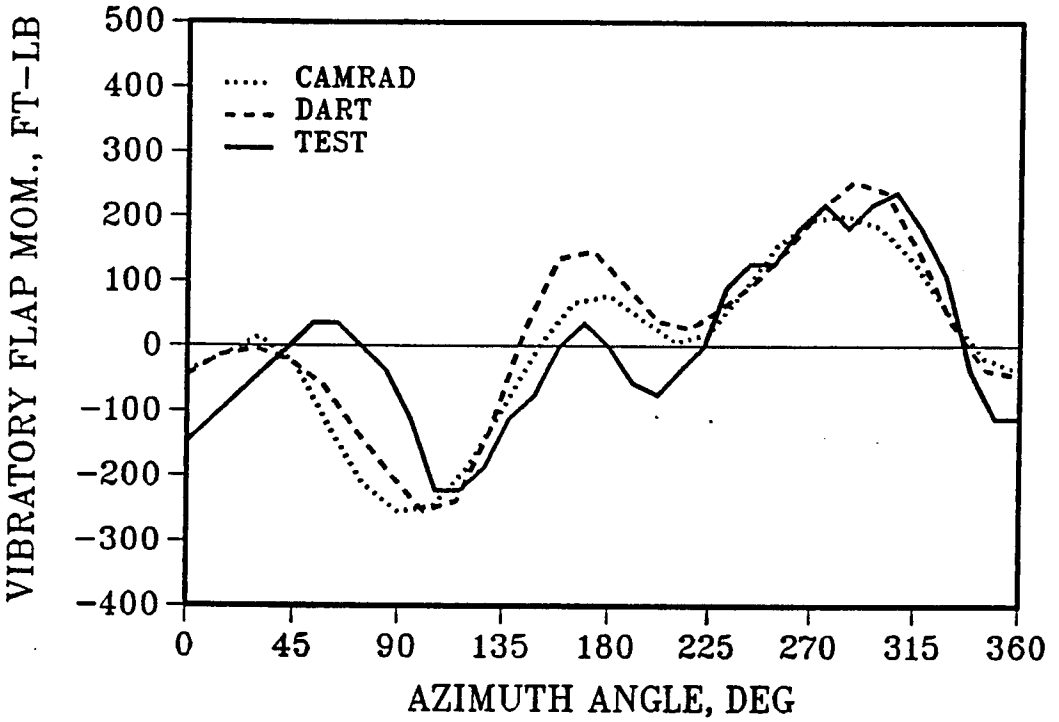

Figure A-2. Flap Bending Time History at .36R – 80 kts.

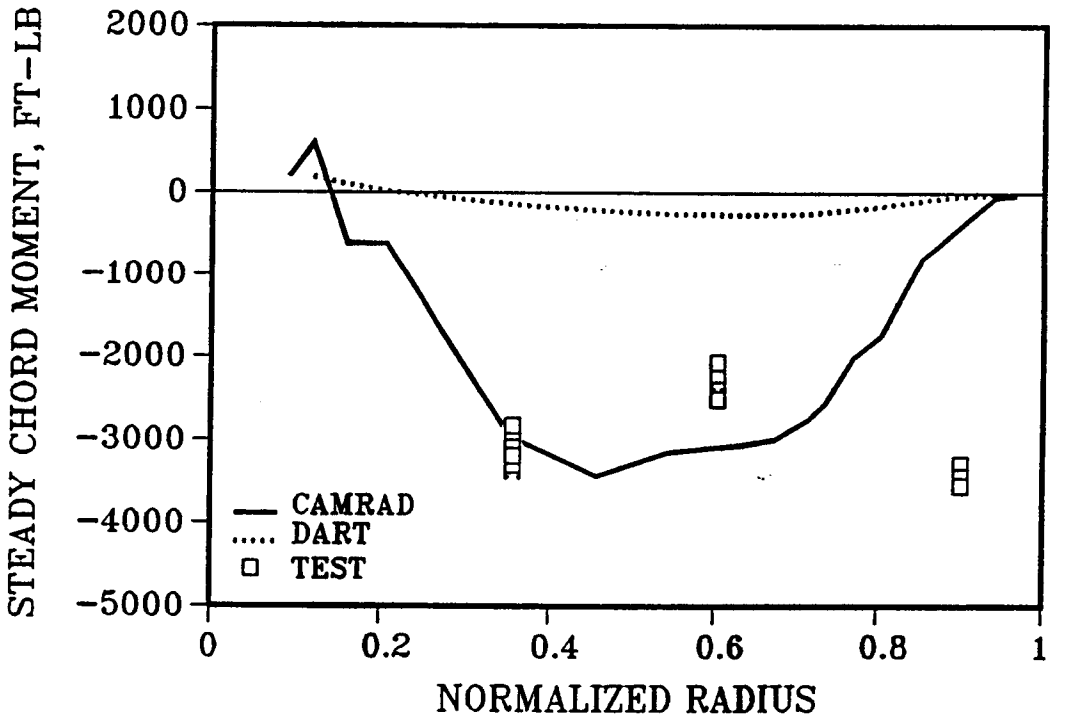

Figure A-3a. Steady Chord Bending Moment vs. Radius – 80 kts.

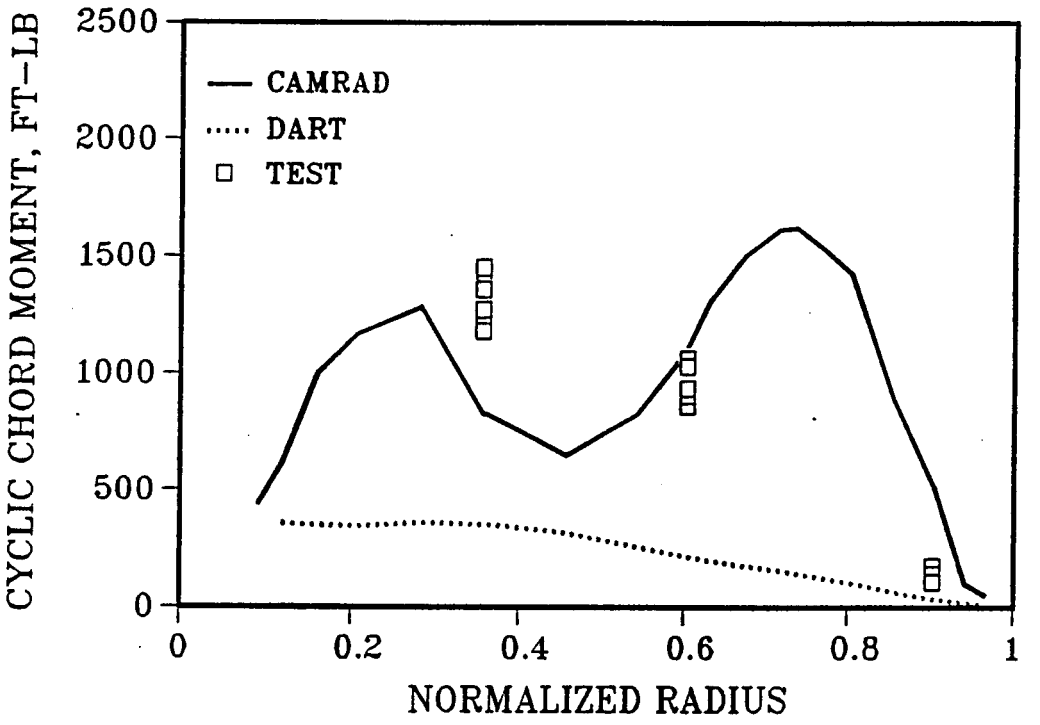

Figure A-3b. Cyclic Chord Bending Moment vs. Radius – 80 kts.

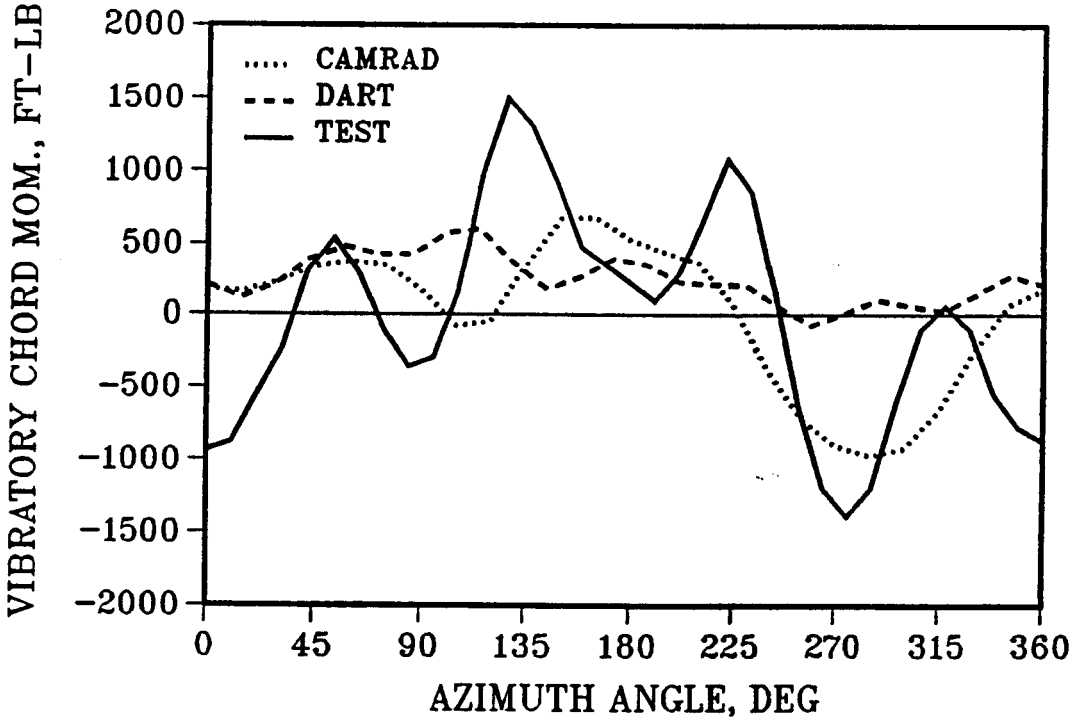

Figure A-4. Chord Bending Time History at .36R – 80 kts.

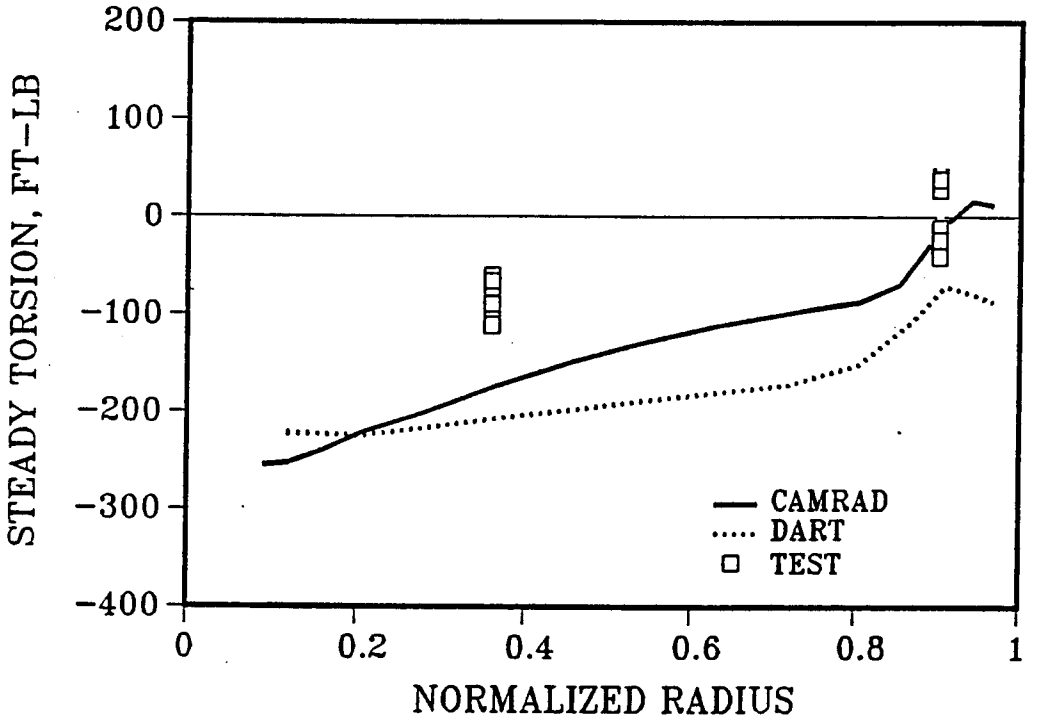

Figure A–5a. Steady Torsion Moment vs. Radius – 80 kts.

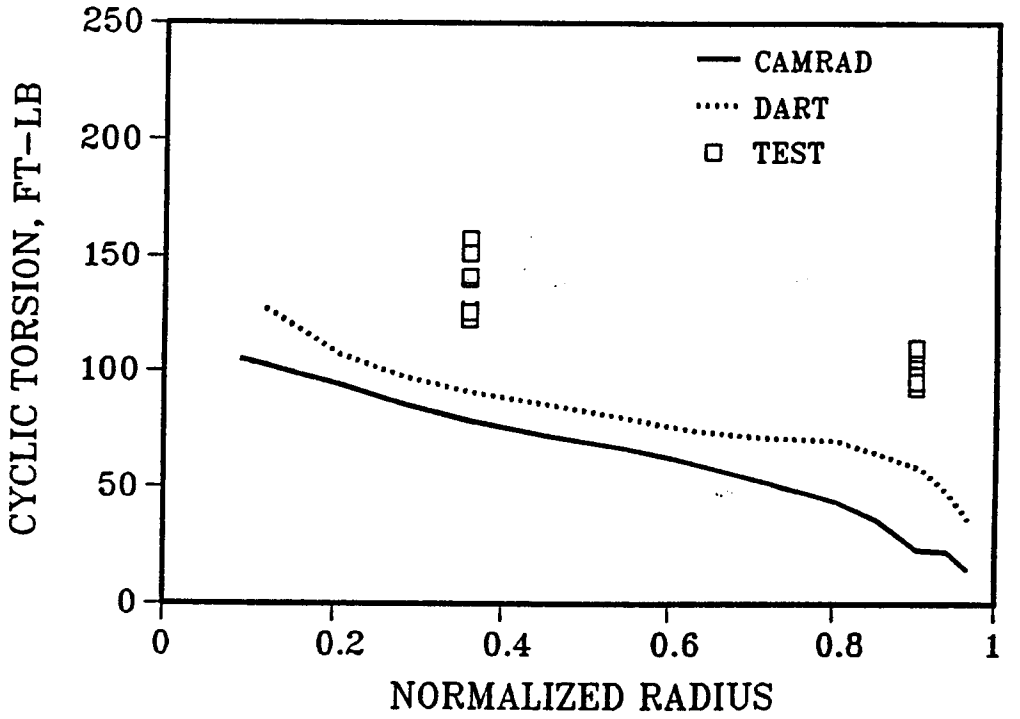

Figure A–5b. Cyclic Torsion Moment vs. Radius – 80 kts.

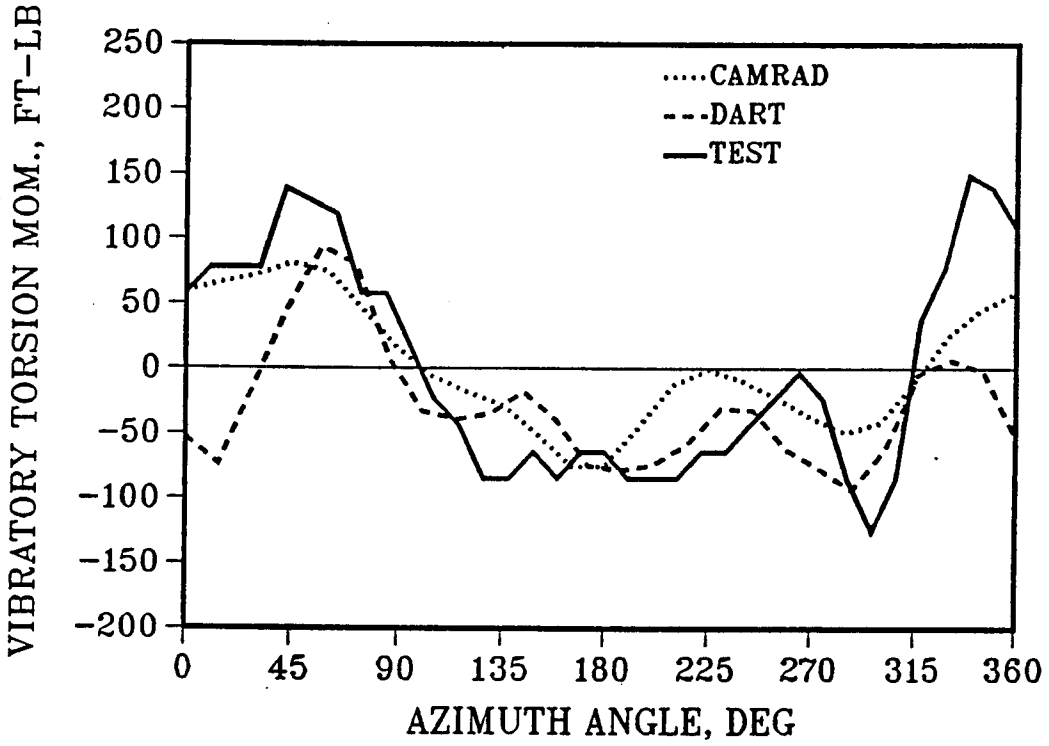

Figure A–6. Torsion Time History at .36R – 80 kts.

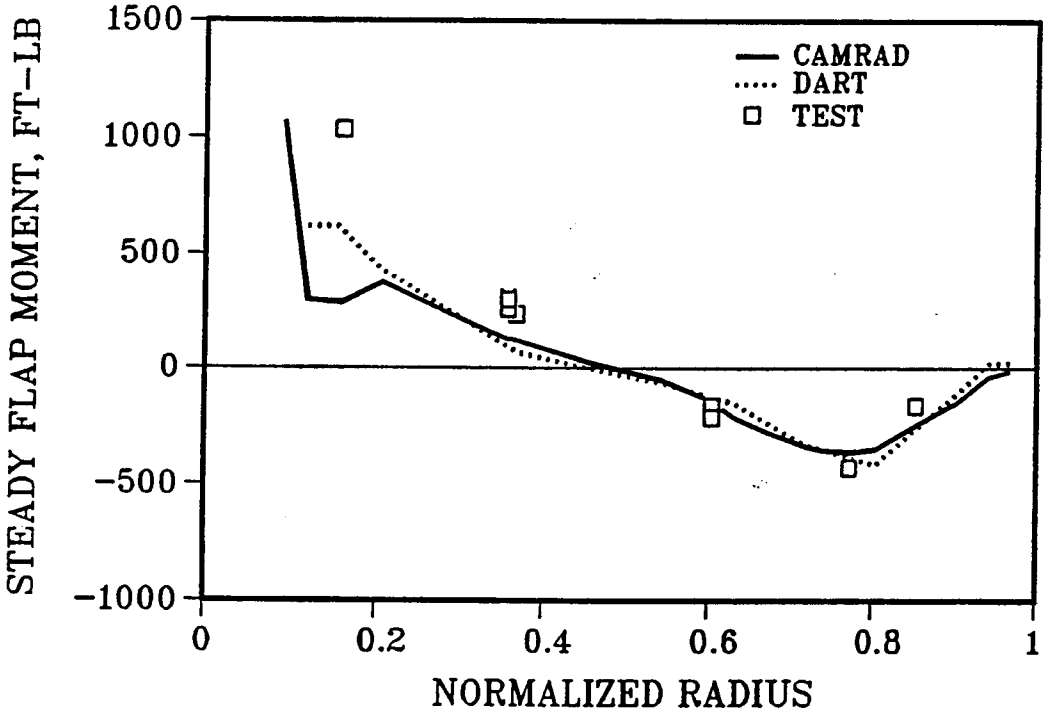

Figure A–7a. Steady Flap Bending Moment vs. Radius – 140 kts.

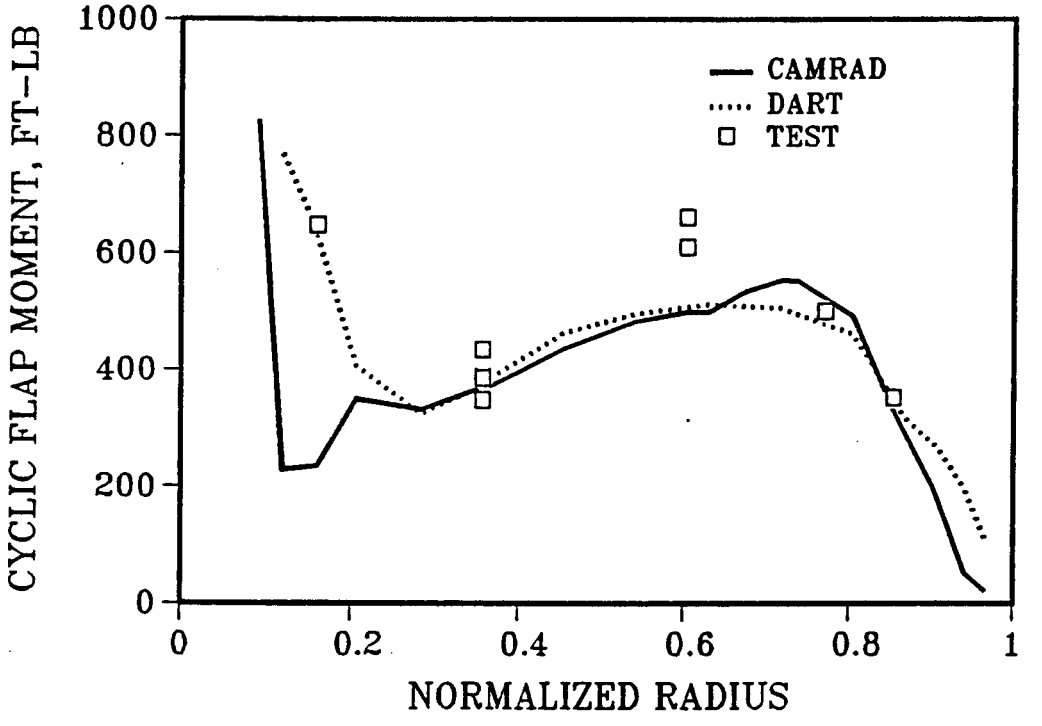

Figure A–7b. Cyclic Flap Bending Moment vs. Radius – 140 kts.

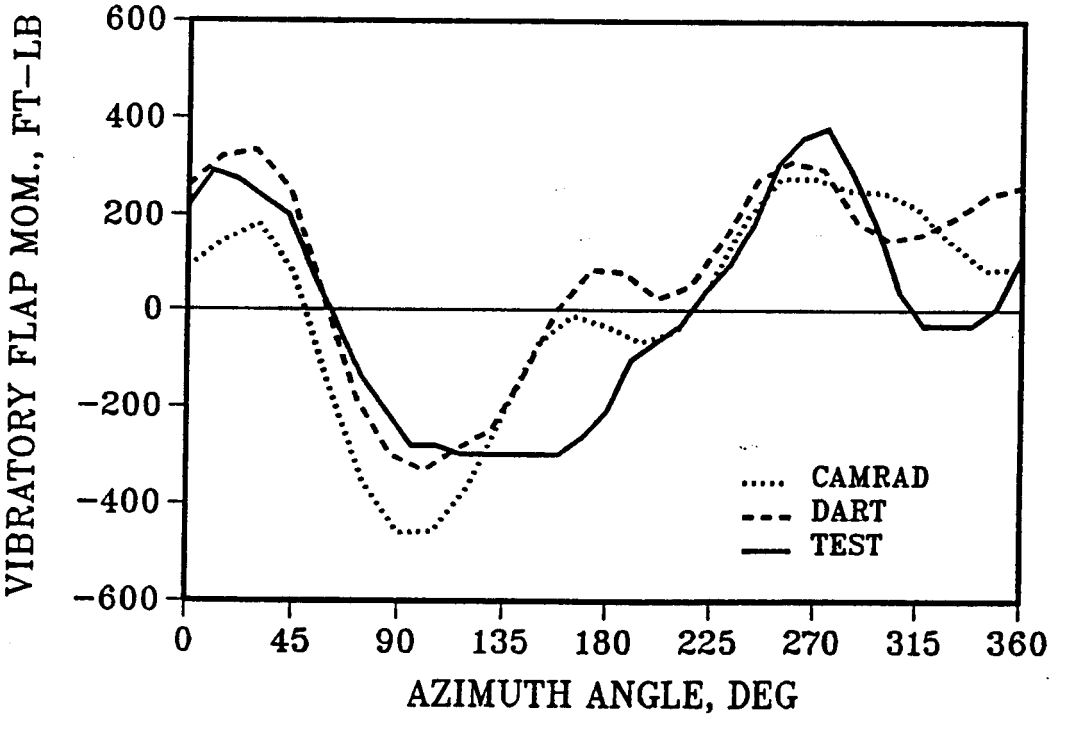

Figure A–8. Flap Bending Time History at .36R – 140 kts.

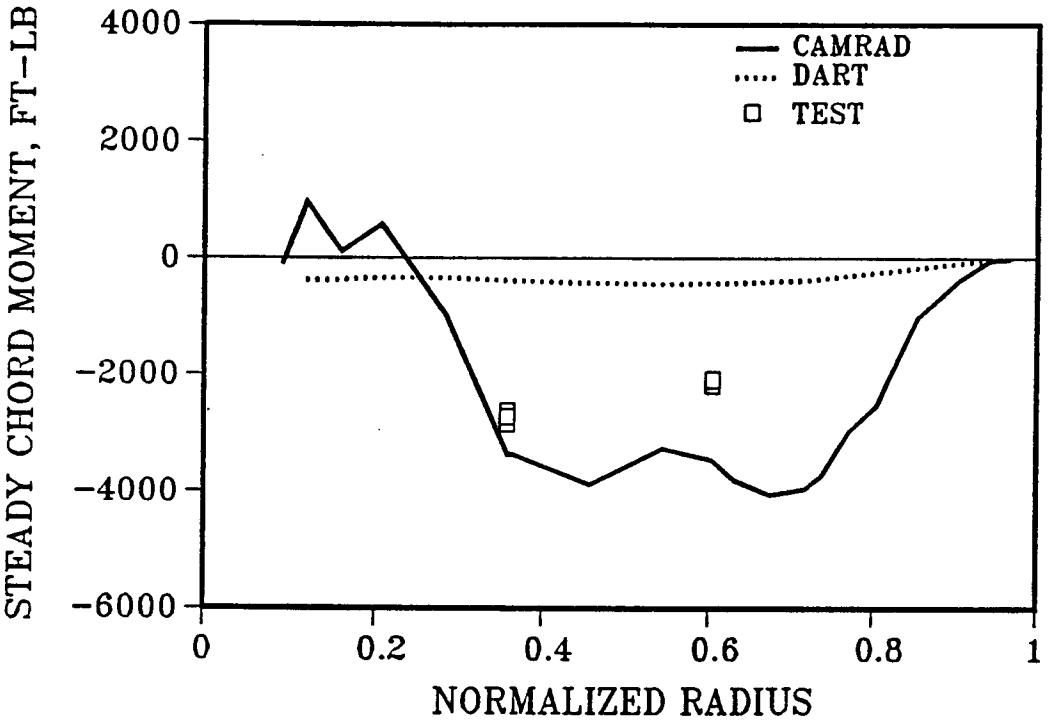

Figure A–9a. Steady Chord Bending Moment vs. Radius – 140 kts

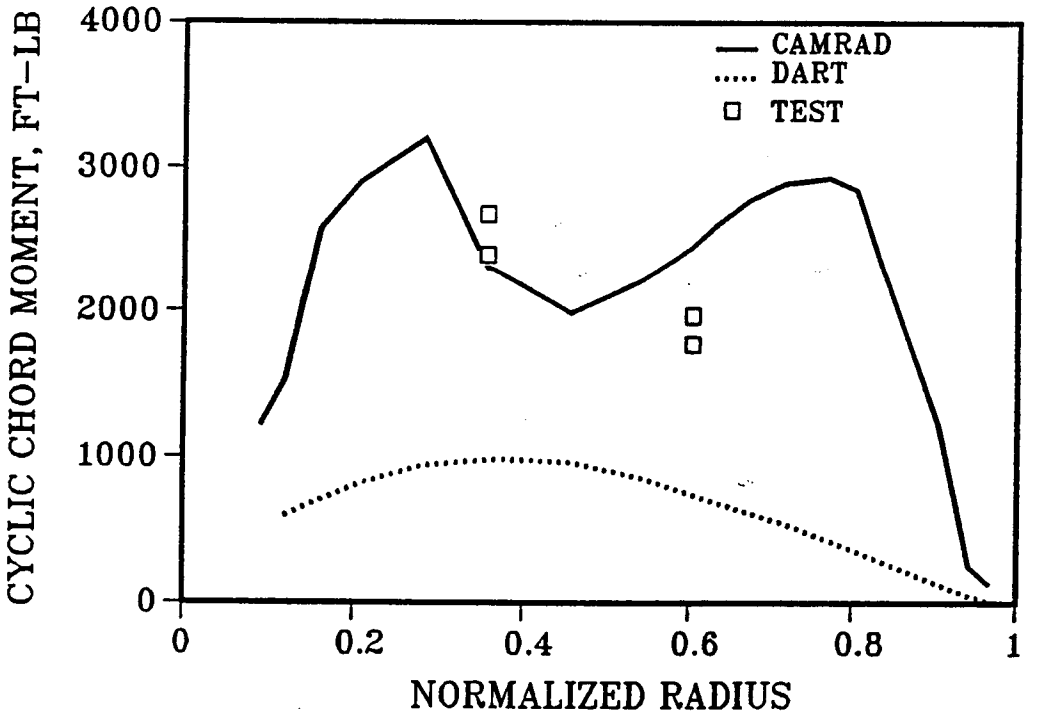

Figure A–9b. Cyclic Chord Bending Moment vs. Radius – 140 kts.

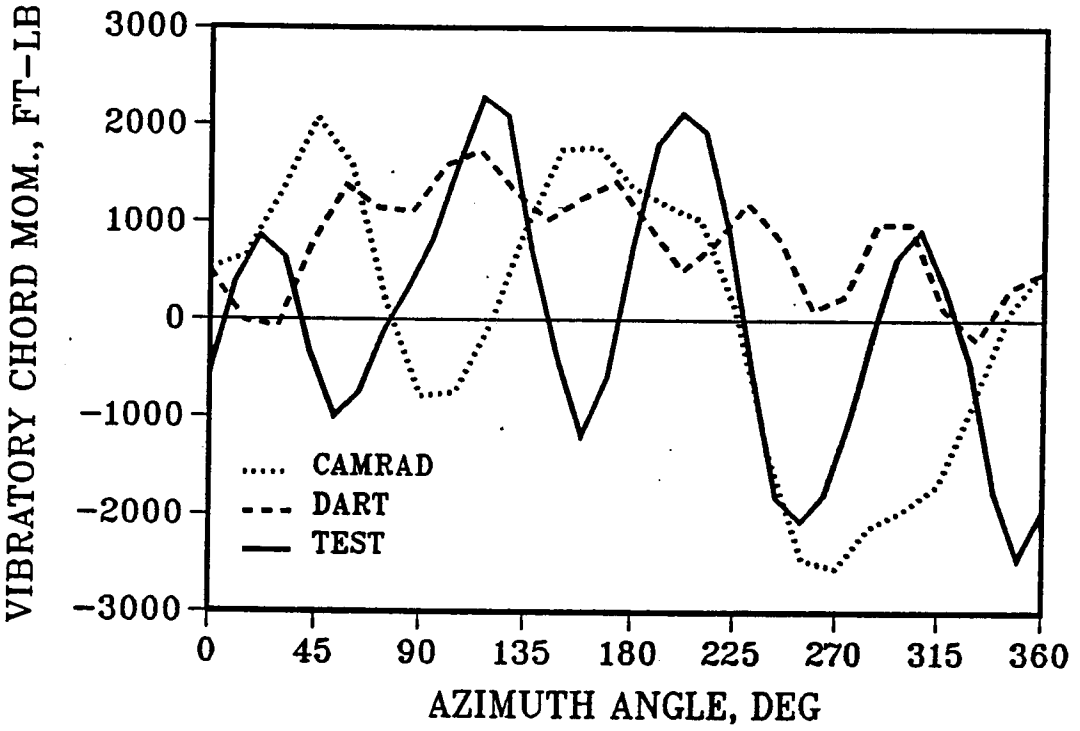

Figure A–10. Chord Bending Time History at .36R – 140 kts.

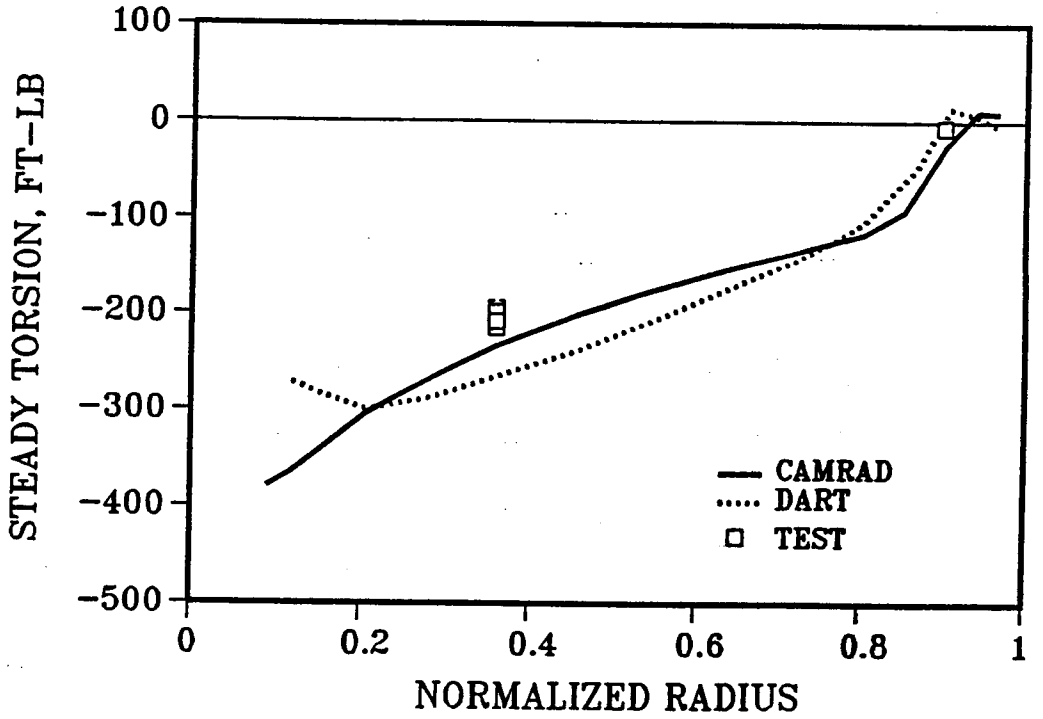

Figure A–11a. Steady Torsion Moment vs. Radius – 140 kts.

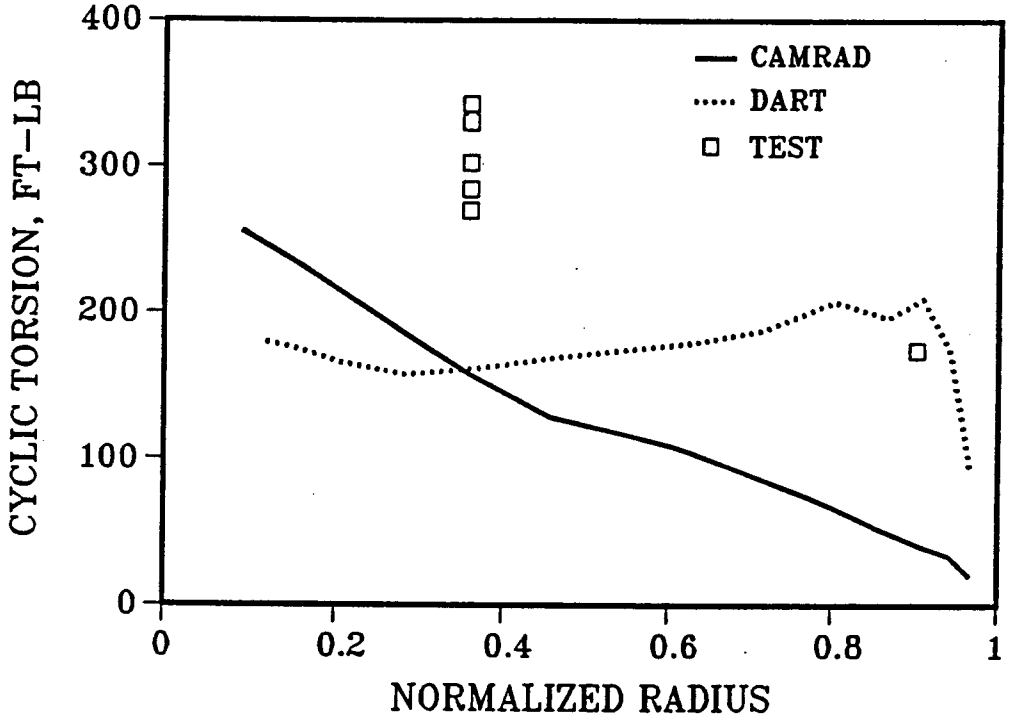

Figure A–11b. Cyclic Torsion Moment vs. Radius – 140 kts.

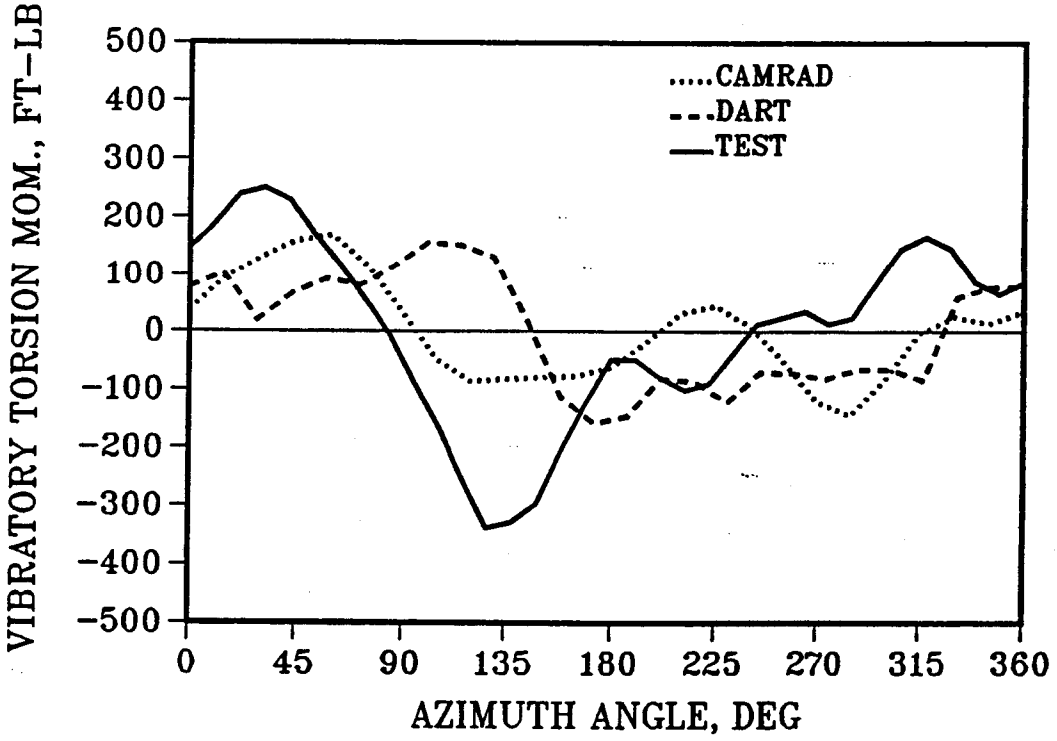

Figure A–12. Torsion Time History at .36R – 140 kts.

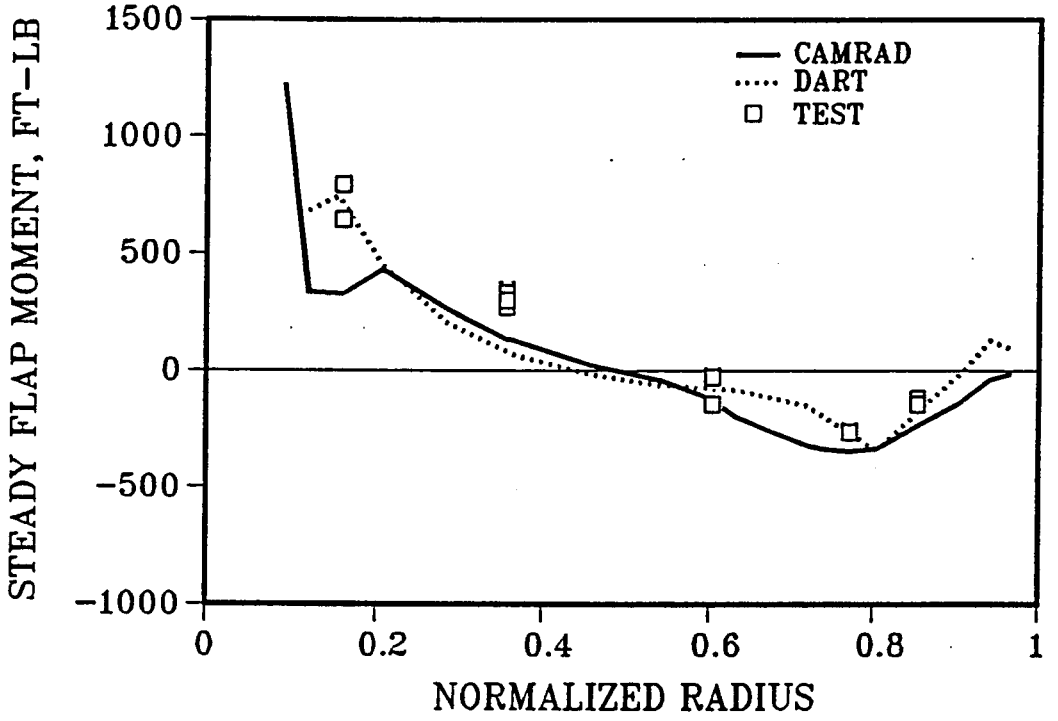

Figure A–13a. Steady Flap Bending Moment vs. Radius – 154 kts.

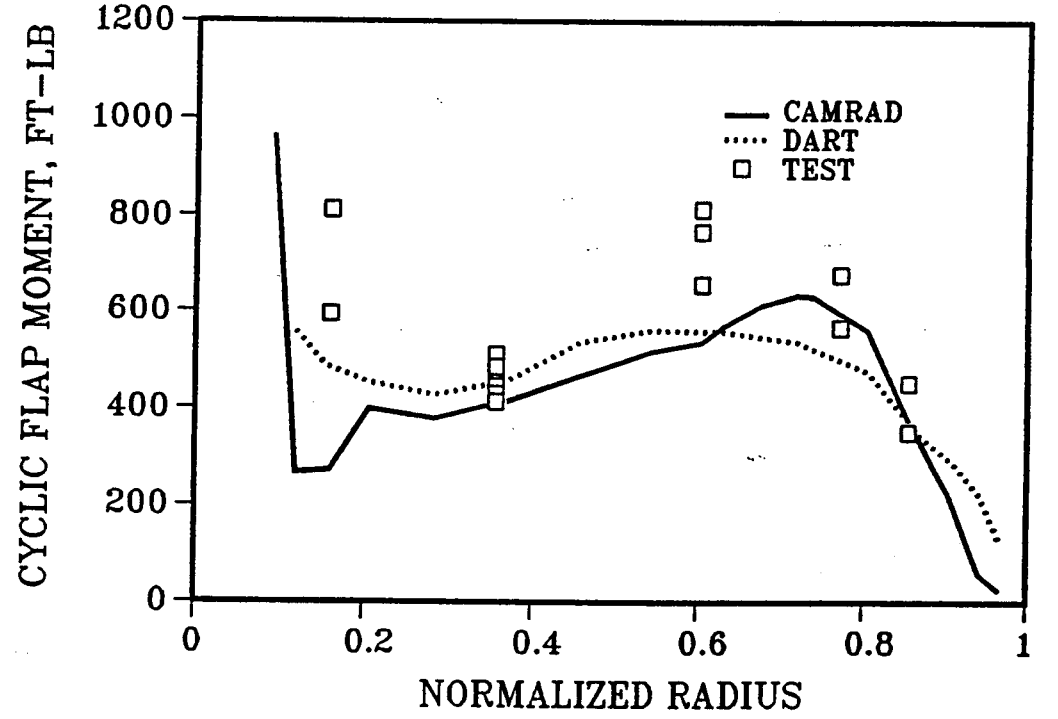

Figure A–13b. Cyclic Flap Bending Moment vs. Radius – 154 kts.

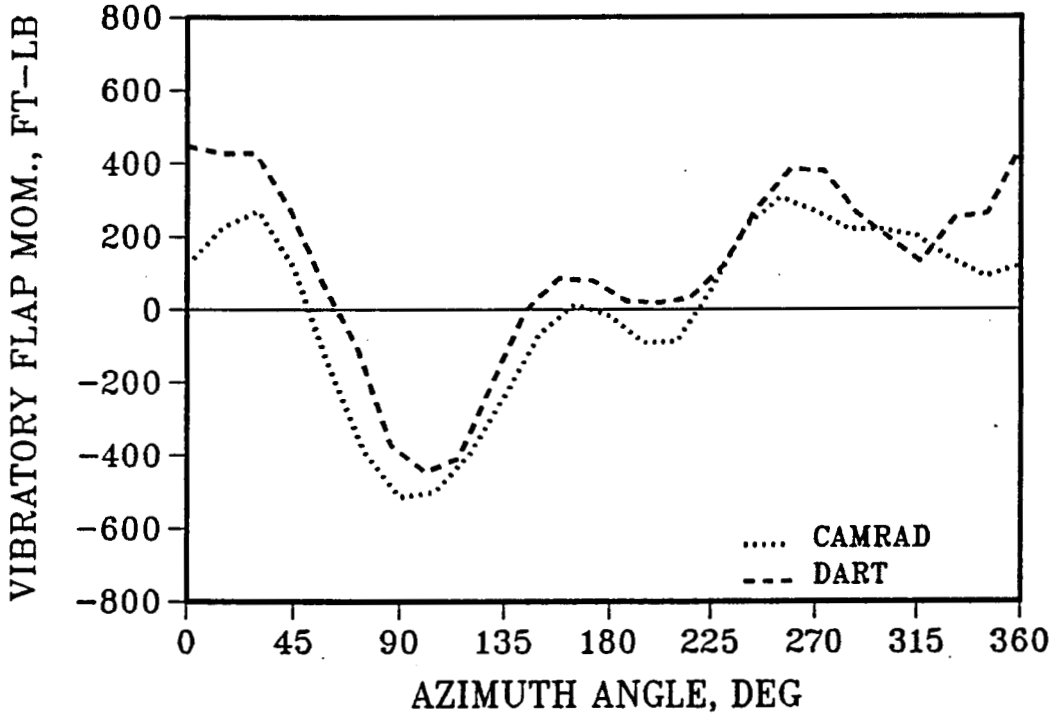

Figure A-14. Flap Bending Time History at .36R – 154 kts.

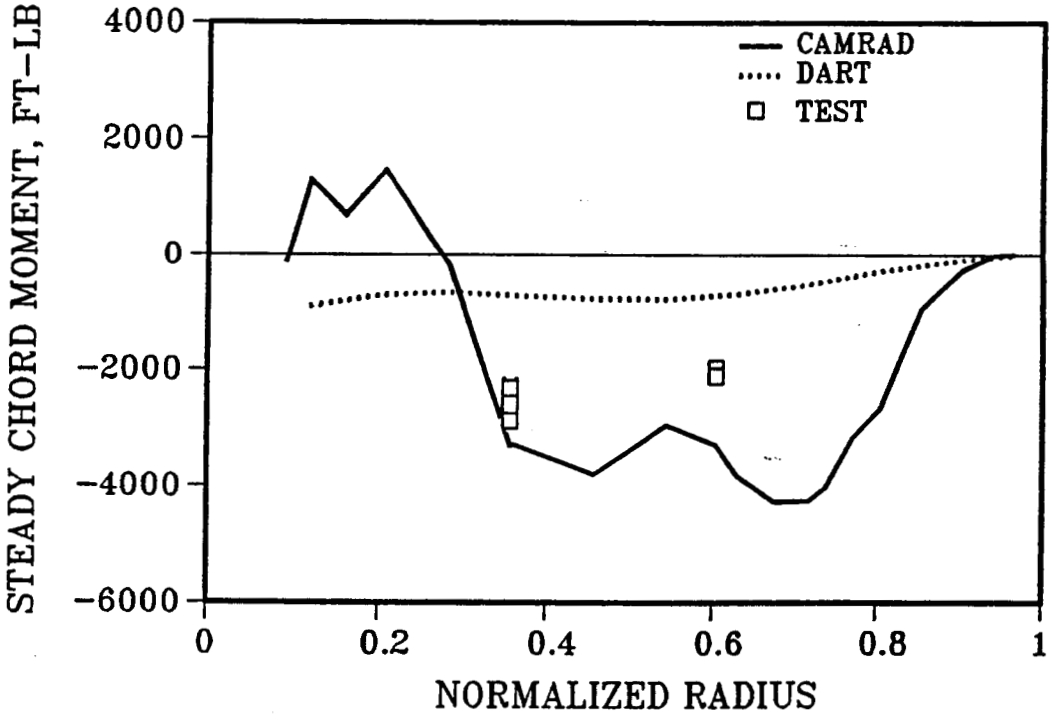

Figure A-15a. Steady Chord Bending Moment vs. Radius – 154 kts

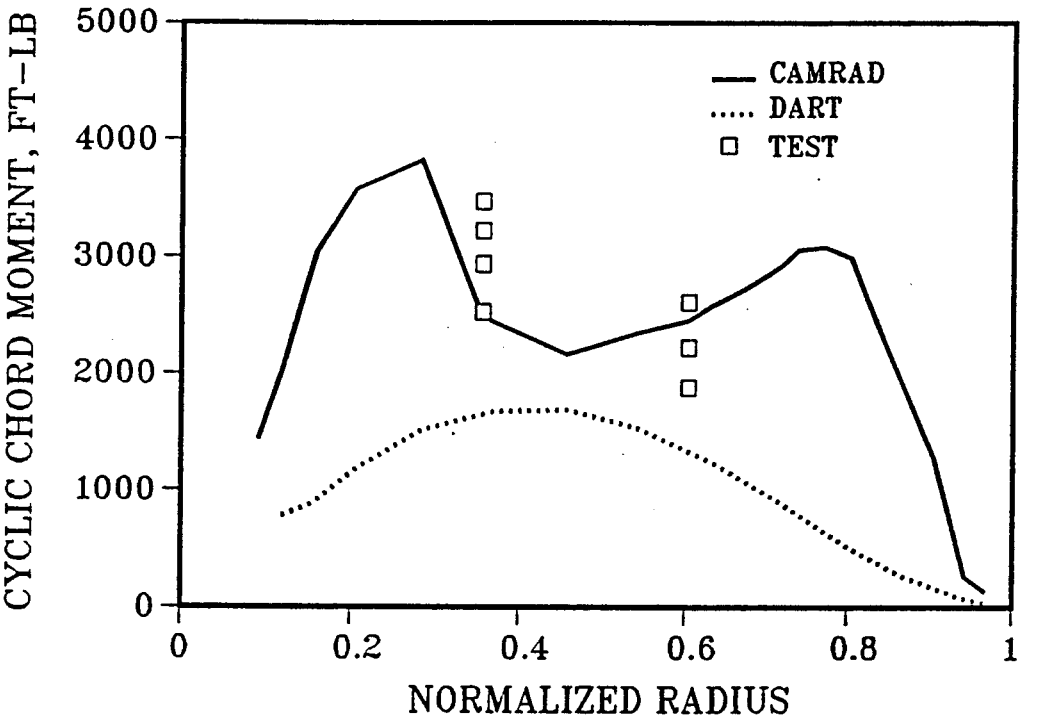

Figure A–15b. Cyclic Chord Bending Moment vs. Radius – 154 kts

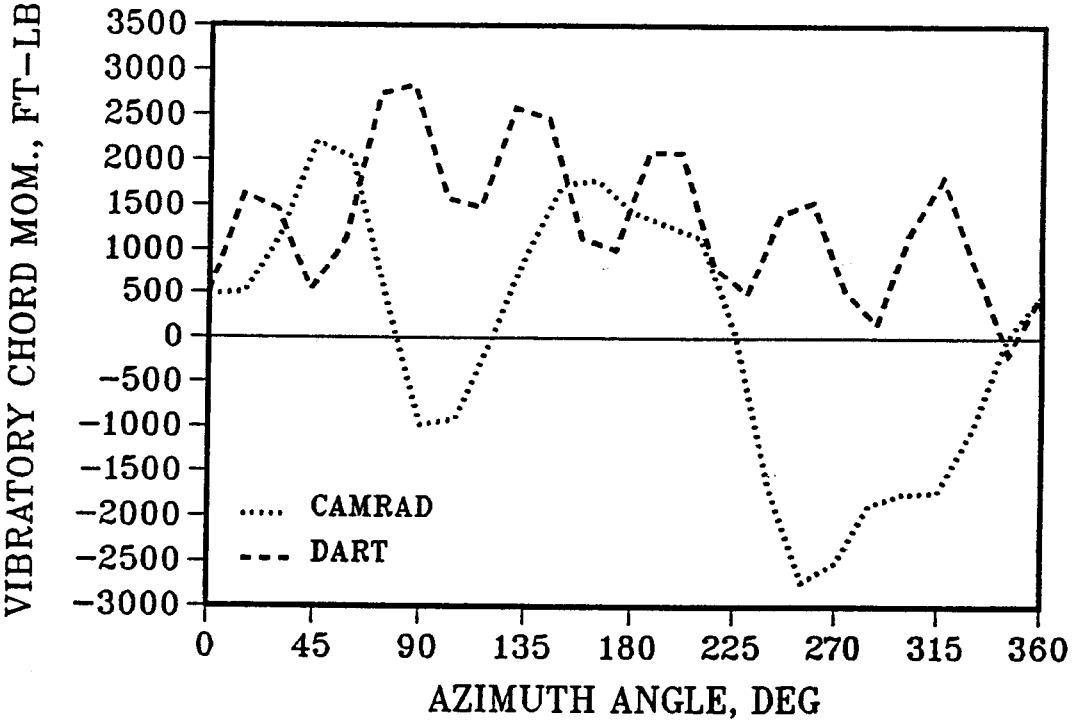

Figure A–16. Chord Bending Time History at .36R – 154 kts.

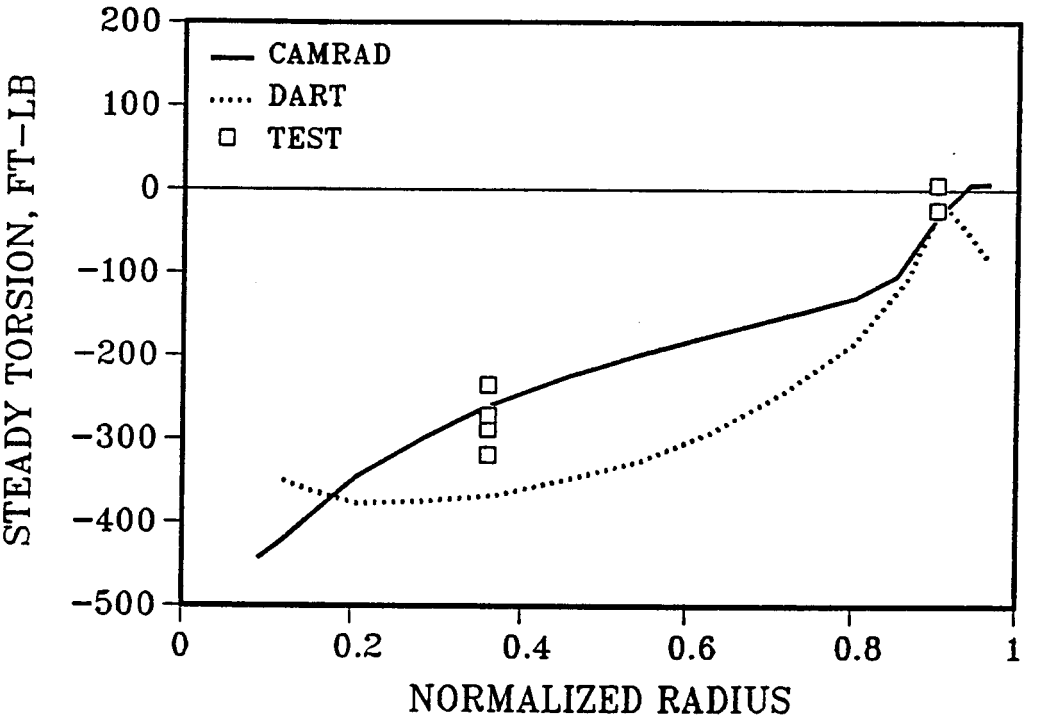

Figure A-17a. Steady Torsion Moment vs. Radius – 154 kts.

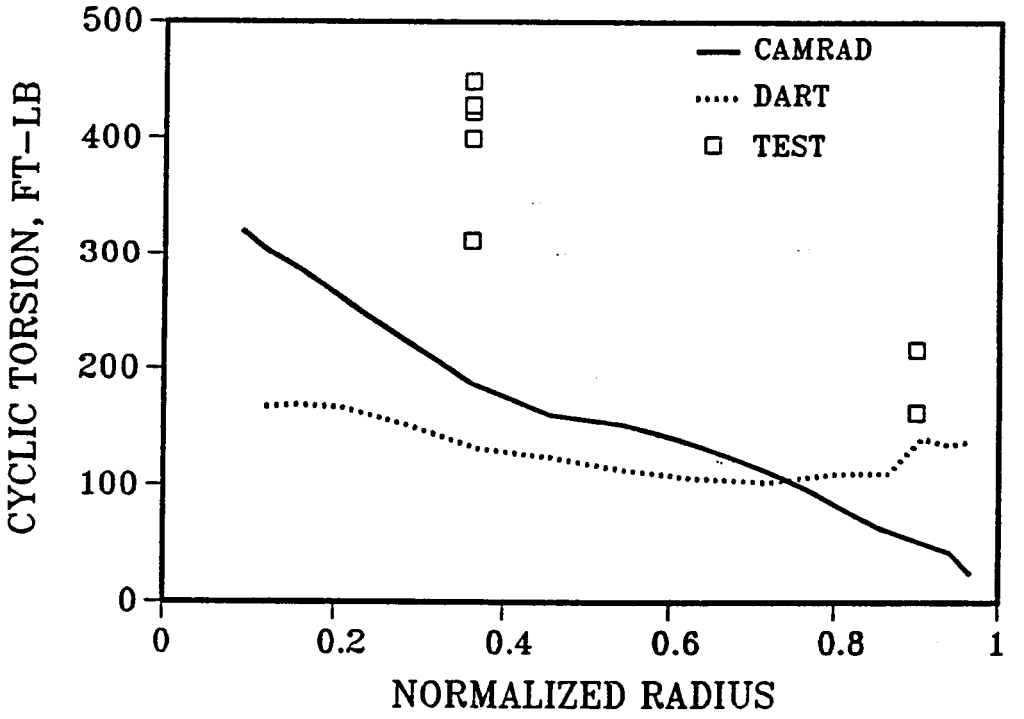

Figure A-17b. Cyclic Torsion Moment vs. Radius – 154 kts.

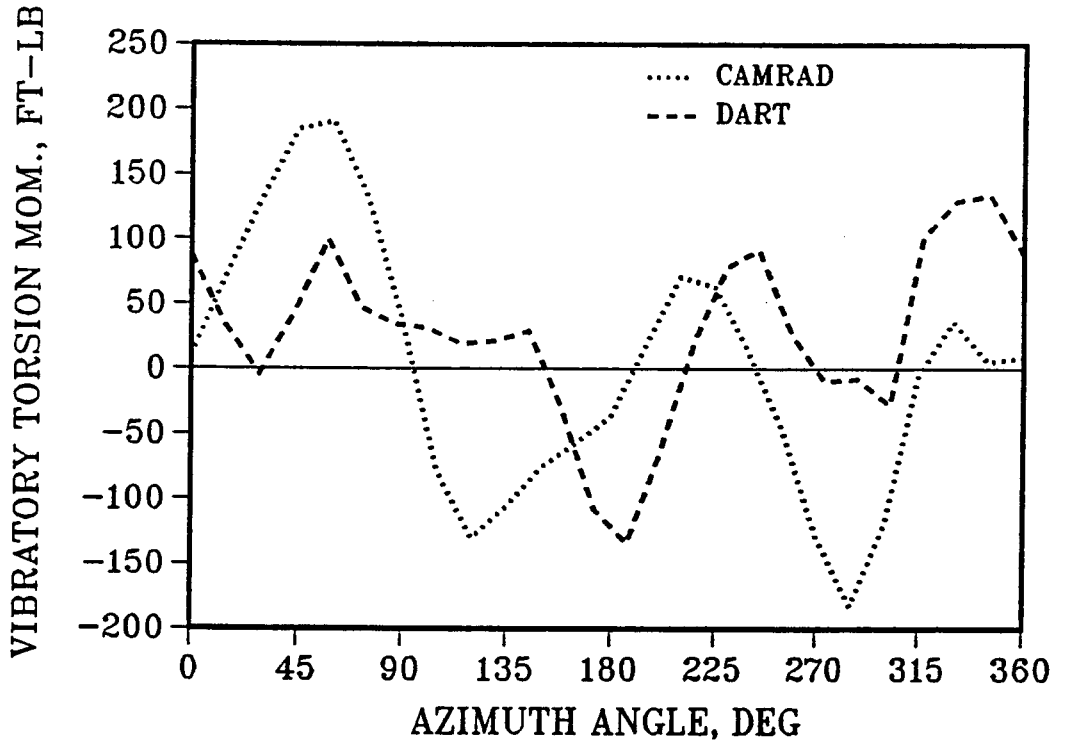

Figure A-18. Torsion Time History at .36R – 154 kts.

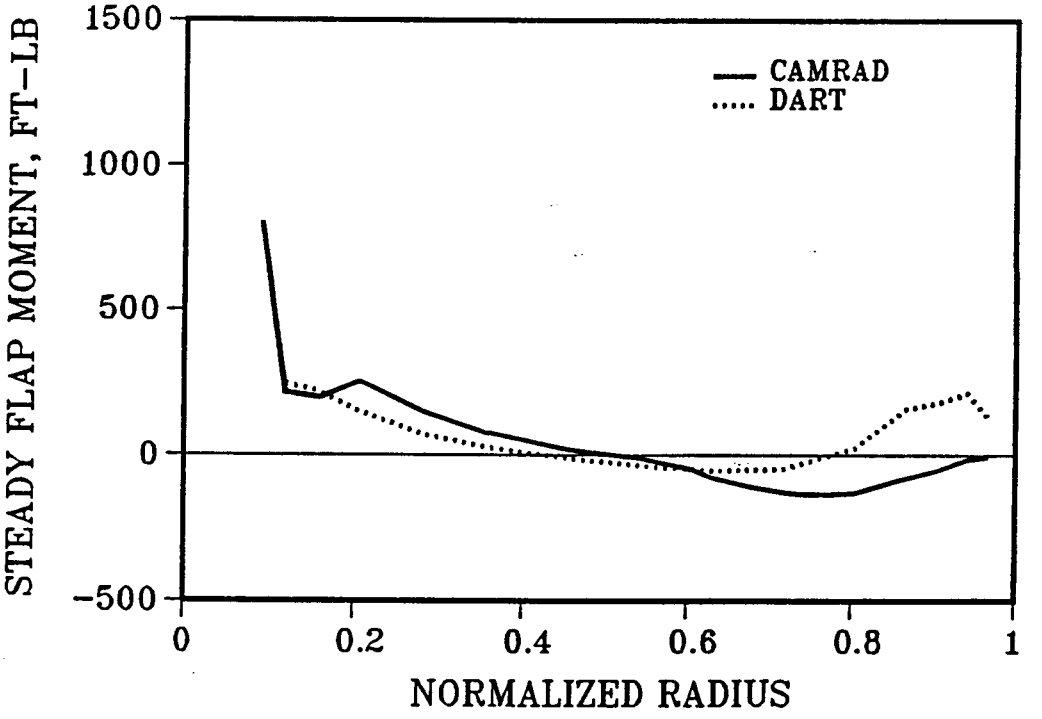

Figure A-19a. Steady Flap Bending Moment vs. Radius – Hover

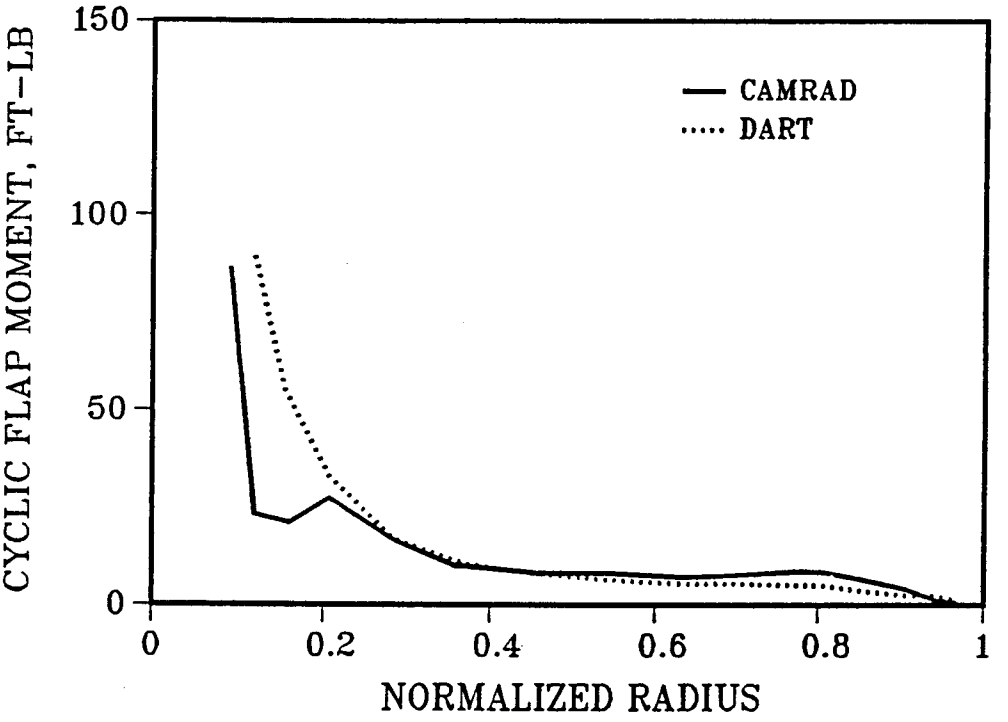

Figure A-19b. Cyclic Flap Bending Moment vs. Radius – Hover

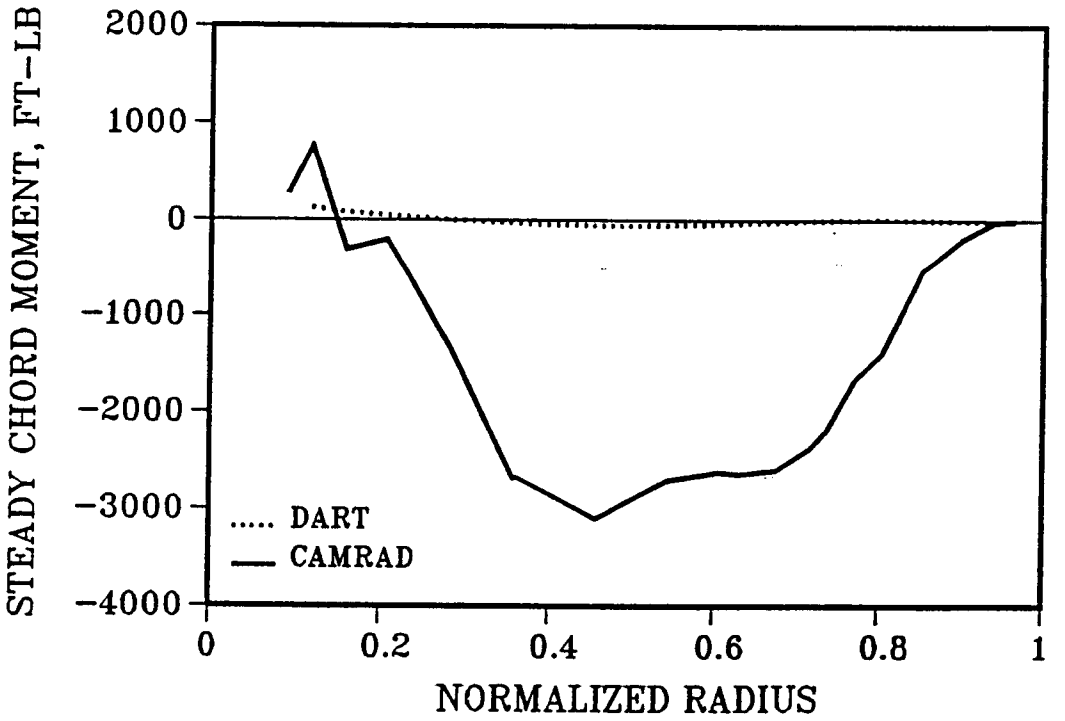

Figure A-20a. Steady Chord Bending Moment vs. Radius – Hover

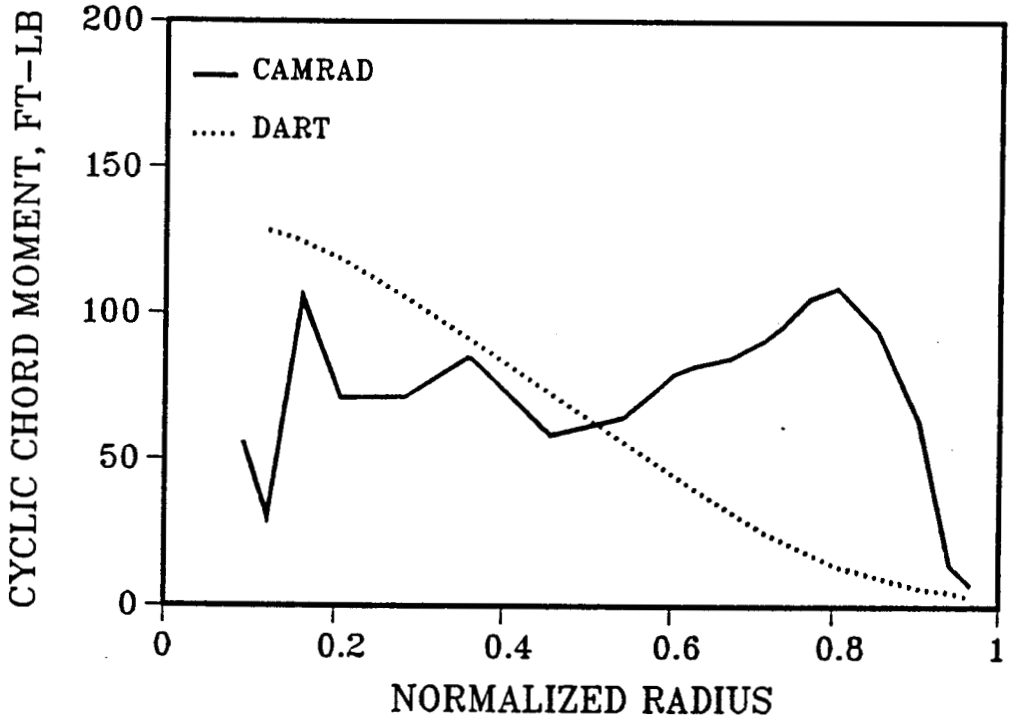

Figure A–20b. Cyclic Chord Bending Moment vs. Radius – Hover

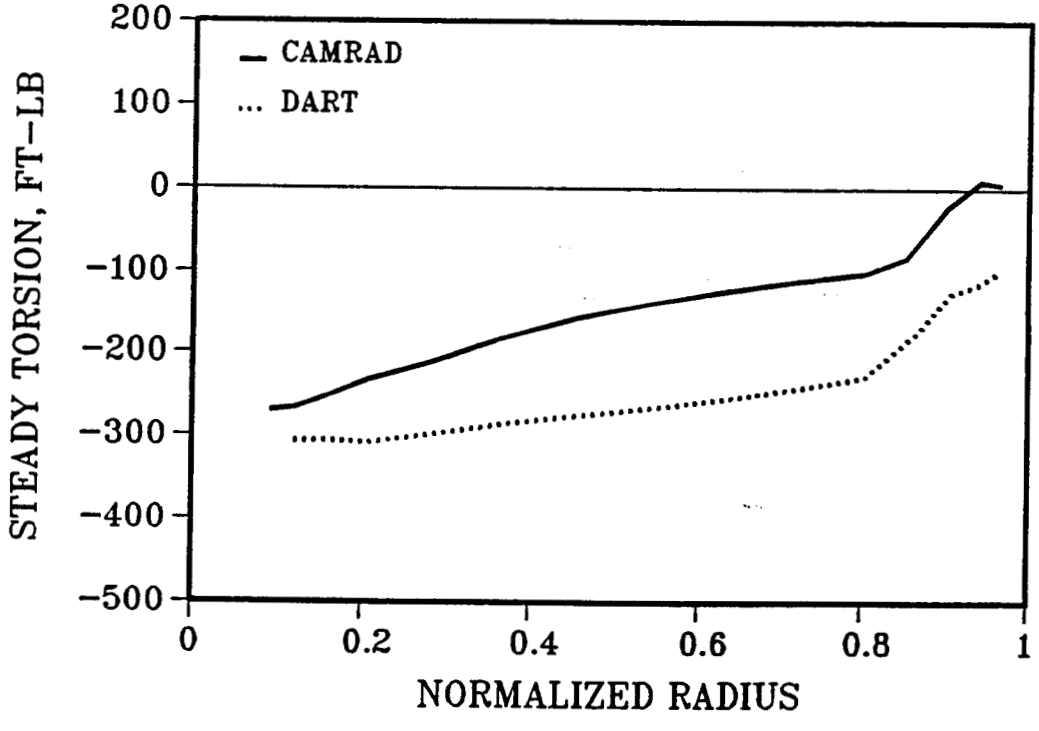

Figure A–21a. Steady Torsion Moment vs. Radius – Hover

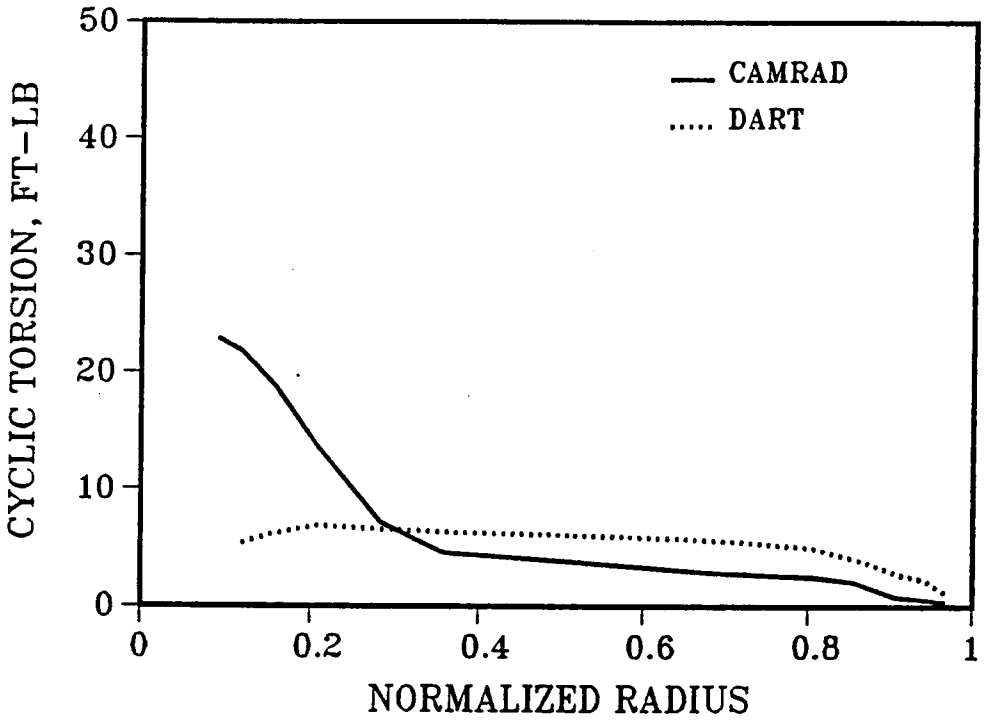

Figure A–21b. Cyclic Torsion Moment vs. Radius – Hover

NASA National Aeronautics and Space Administration

Report Documentation Page

1. Report No.	2. Government Accession No.	3. Recipient's Catalog No.
NASA CR-177455		

4. Title and Subtitle
Application of a Comprehensive Analytical Model of Rotor Aerodynamics and Dynamics (CAMRAD) to the McDonnell Douglas AH-64A Helicopter

5. Report Date
November 1988

6. Performing Organization Code

7. Author(s)
Cynthia B. Callahan
Duane E. Bassett

8. Performing Organization Report No.

10. Work Unit No.
505-61-5

9. Performing Organization Name and Address
McDonnell Douglas Helicopter Company
Mesa, AZ 85205

11. Contract or Grant No.
A63622C

13. Type of Report and Period Covered
Contractor Report, Final

12. Sponsoring Agency Name and Address
Ames Research Center
Moffett Field, CA 94035

14. Sponsoring Agency Code

15. Supplementary Notes
Point of Contact: Edward I. Seto
FHI, M/S 237-5
Moffett Field, CA 94035
(415) 694-5664

16. Abstract
A model of the McDonnell Douglas Helicopter Company (MDHC) AH-64A helicopter was generated in a Comprehensive Analytical Model of Rotorcraft Aerodynamics and Dynamics (CAMRAD) in an effort to validate its analytical capabilities for modeling a current advanced Army helicopter. The initial phase of the effort involved the generation of CAMRAD input files necessary for the complete aerodynamic, structural and dynamic definition of the production AH-64A helicopter. The input files were checked by making comparisons of CAMRAD full helciopter trim and main rotor blade natural frequency predictions with those of MDHC's full helicopter trim program, Blade Element Trim (BETRIM), and dynamic analysis code, Dynamic Analysis Research Tool (DART), respectively. The main thrust of the study concerned the application of the AH-64A CAMRAD model thus developed and verified for main rotor blade structural loads predictions and comparison with DART analytical results. The investigation provided insight not only into the usefulness of CAMRAD for the AH-64A performance and dynamics prediction, but also into the limitations of the program for modeling advanced rotor and fuselage systems. This report discusses the model development effort, presents the results of the CAMRAD correlation studies, and offers some general conclusions on the applicability of CAMRAD for rotor aeroelastic loads prediction for current and future rotorcraft configurations.

17. Key Words (Suggested by Author(s))	18. Distribution Statement
Helicopter Analysis CAMRAD DART, BETRIM Rotor Aerodynamics Rotor Dynamics AH-64A	Unclassified-Unlimited Subject Category-02

19. Security Classif. (of this report)	20. Security Classif. (of this page)	21. No. of pages	22. Price
Unclassified	Unclassifed	60	AD4

PREPARATION OF THE REPORT DOCUMENTATION PAGE

The last page of a report facing the third cover is the Report Documentation Page, RDP. Information presented on this page is used in announcing and cataloging reports as well as preparing the cover and title page. Thus it is important that the information be correct. Instructions for filling in each block of the form are as follows:

Block 1. Report No. NASA report series number, if preassigned.

Block 2. Government Accession No. Leave blank.

Block 3. Recipient's Catalog No. Reserved for use by each report recipient.

Block 4. Title and Subtitle. Typed in caps and lower case with dash or period separating subtitle from title.

Block 5. Report Date. Approximate month and year the report will be published.

Block 6. Performing Organization Code. Leave blank.

Block 7. Author(s). Provide full names exactly as they are to appear on the title page. If applicable, the word editor should follow a name.

Block 8. Performing Organization Report No. NASA installation report control number and, if desired, the non-NASA performing organization report control number.

Block 9. Performing Organization Name and Address. Provide affiliation (NASA program office, NASA installation, or contractor name) of authors.

Block 10. Work Unit No. Provide Research and Technology Objectives and Plans (RTOP) number.

Block 11. Contract or Grant No. Provide when applicable.

Block 12. Sponsoring Agency Name and Address. National Aeronautics and Space Administration, Washington, D.C. 20546-0001. If contractor report, add NASA installation or HQ program office.

Block 13. Type of Report and Period Covered. NASA formal report series; for Contractor Report also list type (interim, final) and period covered when applicable.

Block 14. Sponsoring Agency Code. Leave blank.

Block 15. Supplementary Notes. Information not included elsewhere: affiliation of authors if additional space is required for block 9, notice of work sponsored by another agency, monitor of contract, information about supplements (film, data tapes, etc.), meeting site and date for presented papers, journal to which an article has been submitted, note of a report made from a thesis, appendix by author other than shown in block 7.

Block 16. Abstract. The abstract should be informative rather than descriptive and should state the objectives of the investigation, the methods employed (e.g., simulation, experiment, or remote sensing), the results obtained, and the conclusions reached.

Block 17. Key Words. Identifying words or phrases to be used in cataloging the report.

Block 18. Distribution Statement. Indicate whether report is available to public or not. If not to be controlled, use "Unclassified-Unlimited." If controlled availability is required, list the category approved on the Document Availability Authorization Form (see NHB 2200.2, Form FF427). Also specify subject category (see "Table of Contents" in a current issue of STAR), in which report is to be distributed.

Block 19. Security Classification (of this report). Self-explanatory.

Block 20. Security Classification (of this page). Self-explanatory.

Block 21. No. of Pages. Count front matter pages beginning with iii, text pages including internal blank pages, and the RDP, but not the title page or the back of the title page.

Block 22. Price Code. If block 18 shows "Unclassified-Unlimited," provide the NTIS price code (see "NTIS Price Schedules" in a current issue of STAR) and at the bottom of the form add either "For sale by the National Technical Information Service, Springfield, VA 22161-2171" or "For sale by the Superintendent of Documents, U.S. Government Printing Office, Washington, DC 20402-0001," whichever is appropriate.